Mechanisms of action that contribute to the efficacy of ivy leaves dry extract EA 575®

Dissertation

zur

Erlangung des Doktorgrades (Dr. rer. nat.)

der

Mathematisch-Naturwissenschaftlichen Fakultät

der

Rheinischen Friedrich-Wilhelms-Universität Bonn

vorgelegt von

Janka Schulte-Michels

aus

Bonn

Bonn 2018

Angefertigt mit Genehmigung der Mathematisch-Naturwissenschaftlichen Fakultät
der Rheinischen Friedrich-Wilhelms-Universität Bonn.

.

1. Gutachter: Prof. Dr. H. Häberlein

2. Gutachter: Prof. Dr. E. Kostenis

Tag der Promotion: 27.11.2018

Erscheinungsjahr 2018

Στην μνήμη της μαμάς μου, δεν θα σε ξεχάσω ποτέ!

„Wissen ist Nacht“ – Prof. Dr. Abdul Nachtigaller

Abstract

The ivy leaves dry extract EA 575® is an approved cough remedy distributed in more than 100 countries worldwide.

The modes of action for its bronchospasmolytic, secretolytic, and anti-inflammatory effects remain poorly understood. Therefore, this work focuses on a contribution to these mechanisms.

Within this work it is shown that the former investigated inhibition of β_2-adrenergic receptor internalization arrives from an indirect inhibition of receptor phosphorylation by GRK2. Also the recruitment of β-arrestin2 to the β_2-adrenergic receptor (β_2AR) is shown to be diminished after EA 575® pre-treatment under stimulating conditions.

With respect to anti-inflammatory effects, EA 575® reduces IL-6 secretion from murine macrophages after LPS stimulation. This effect is explained by a reduced NFκB transcriptional activity measured by a reporter gene assay based on luciferase activity in HEK and THP-1 cells. As assessed by immunostaining, the translocation of NFκB into the nucleus under stimulating conditions is also impaired, which is explained by a higher amount of bound NFκB to its inhibitor IκBα detected by a protein fragment complementation assay. This result is underlined with a lowered phosphorylation of IκBα and a heightened phosphorylation of NFκB subunit RelA at Ser536 after EA 575® pre-treatment and TNFα stimulation.

Finally, it is demonstrated in HEK Nanoluc-PEST cells that NFκB transcriptional activity is diminished by β_2-adrenergic stimulation and synergistically inhibited by EA 575® pre-incubation. Interestingly, this effect is shown to be β-arrestin dependent. Whether or not this crosstalk contributes to the efficacy of EA 575® requires further investigation.

Table of content

List of abbreviations

β_2AR	β_2-adrenergic receptor
β-gal	β-galactosidase
cAMP	cyclic adenosine-3',5'-monophosphate
CHO	Chinese hamster ovarian
CID	Compound identification
Cys	Cysteine
DCA	Dicaffeoylquinic acid
DMEM	Dulbecco's modified eagle medium
DNA	Deoxyribonucleic acid
EFC	Enzyme fragment complementation
FCS	Fetal calf serum
GFP	Green fluorescent protein
GPCR	G-protein coupled receptor
GRK	G-protein coupled receptor kinase
GUV	Giant unilamellar vesicle
HBSS	Hanks balanced salt solution
HEK	Human embryonic kidney
HEPES	4-(2-hydroxyethyl)-1-piperazineethanesulfonic acid
HPLC	High pressure liquid chromatography
Hygro	Hygromycin
IFNγ	Interferon gamma
IL	Interleukin

IκB	Inhibitor of nuclear factor 'kappa-light-chain-enhancer' of activated B-cells
KO	Knock out
LB	Lysogeny broth
LPS	Lipopolysaccharide
ns	not significant
NA	Numerical aperture
Nanoluc-PEST	Nanoluciferase destabilized through proline (P), glutamate (E), serine (S), and threonine (T)
NFκB	Nuclear factor ‘kappa-light-chain-enhancer’ of activated B-cells
NIR	Near-infrared
PBS	Phosphate-buffered saline
PFC	Protein fragment complementation
PDL	Poly-D-lysine
PGE1	Prostaglandin E1
P/S	Penicillin/Streptomycin
PTFE	Polytetrafluoroethylene
Rcf	Relative centrifugal force
RelA	v-rel avian reticuloendotheliosis viral oncogene homolog A
RP	Reversed phase

RPMI 1640	Roswell Park Memorial Institute 1640 Medium
Ser	Serine
TBS	Tris-buffered saline
TAE	Tris, acetic acid, EDTA
TNFα	Tumor necrosis factor α
Tyr	Tyrosine
Zeo	Zeocin

List of figures

List of tables

1. Introduction

The ivy leaves dry extract EA 575® is used for the treatment of acute inflammations of the airways associated with cough and for the improvement of symptoms in chronic inflammatory bronchial diseases.

Its bronchospasmolytic and secretolytic effects have been demonstrated in clinical studies [1, 2]. The mechanism of action is based on increased β_2-adrenergic responsiveness of the airways through inhibited β_2-adrenergic receptor (β_2AR) internalization under stimulating conditions, leading to increased receptor binding and formation of cAMP in alveolar type 2 cells (A549) and human airway smooth muscle (HASM) cells [3]. The molecular mechanism for the inhibited receptor internalization remained unclear.

Besides bronchospasmolytic and secretolytic effects, there is growing evidence for an anti-inflammatory effect of EA 575®. Zeil et al. performed a proof of concept study demonstrating that EA 575® as an add-on is beneficial in the treatment of partial or uncontrolled mild persistent allergic asthma in children [4]. Lung function was improved indicated by increased values of in MEF_{75-25}, MEF_{25} and VC after treatment with EA 575®. As asthma is a chronic inflammatory disease, EA 575® was investigated for possible anti-inflammatory effects. In-vivo it was already shown that a, not further defined, ivy extract exhibited anti-inflammatory properties in carrageenan- and cotton-pellet- induced inflammation in rats [5]. In-vitro studies have so far only engaged with single compounds of ivy leaves dry extracts. For example, rutin was shown to influence the NFκB pathway [6, 7].

The aim of this work was, first, to examine the mode of action in which EA 575® inhibits β_2AR internalization. Therefore, a possible effect of α-hederin on β_2AR phosphorylation at Ser355/356 required for receptor internalization was studied. Additionally, the influence of EA 575® on the recruitment of β-arrestin 2 to the β_2AR was examined.

To investigate the effects of EA 575® on inflammatory processes the following further studies were performed:

1. The secretion of IL-6 from murine macrophages was measured.
2. NFκB translocation into the nucleus was examined.
3. NFκB transcriptional activity was investigated with a reporter gene assay.
4. Phosphorylation of IκBα and NFκB subunit RelA was assessed by western blot.
5. The stability of NFκB:IκBα complex was measured in a protein fragment complementation assay.

Furthermore, the impact of EA 575® on the crosstalk between β_2AR signaling and NFκB pathway and the relevance of β-arrestins in these processes were investigated using NFκB reporter gene assays and protein fragment complementation measurements.

2 Materials

2.1 Table 1: Cell lines

Name	Cell type	Supplied by	Reference number
CHO K1 ADRB2 eXpress cells	Chinese ovarian hamster cells overexpressing β_2AR and β-arrestin2 + β-gal EFC	DiscoverX, Fremont, California, USA	NM_000024
HEK 293	Human embryonic kidney cells	Deutsche Sammlung von Mikroorganismen und Zellkulturen (DSMZ) GmbH Braunschweig, Germany	ACC 305
THP-1	Human acute monocytic leukemia cells	DSMZ	ACC 16
J774.2	BALB/C monocyte macrophages	Sigma-Aldrich, Darmstadt, Germany	85011428

2.2 Table 2: Bought solutions

Name	Abbreviation	Supplied by	Reference number
β-mercaptoethanol		Gibco/Thermo Fisher Scientific, Waltham, Massachusetts, USA	31350010
Dulbecco´s modified eagle medium	DMEM	Gibco	31885049
Dulbecco´s modified eagle medium, without phenol red	DMEM without phenol red	Gibco	31053-028
Draq5	-	Thermo Fisher Scientific	62251
Fetal calf serum	FCS	Gibco	10270
Glutamax 100x	Glutamax	Gibco	35050061
L-Glutamine	-	Gibco	25300054
Hank´s balanced salt solution	HBSS	Gibco	14025050
Nano-Glo® Luciferase Assay system	-	Promega, Madison, Wisconsin, USA	N1120
Novex® mouse IL-6 ELISA kit	-	Thermo Fisher Scientific	KMC0061
Odyssey blocking	-	LI-COR, Lincoln,	927-50000

buffer (TBS)		Nebraska, USA	
Penicillin-streptomycin 10000 U/ml	P/S	Gibco	15140122
Phosphate buffered saline	PBS	Gibco	10010056
REVERT LI-COR total protein stain kit	REVERT	LI-COR	926-11016
Roswell Park Memorial Institute 1640 Medium	RPMI	Gibco	31870-025
Sapphire700	-	LI-COR	928-40022
Trypsin EDTA 0.05 %, phenol red	Trypsin	Gibco	25300104

2.3 Table 3: Self-made solutions

Name	Abbreviation	Composition
2x HEPES buffered saline	2xHBS	42 mM HEPES 274 mM NaCl 10 mM KCl 1.4 mM Na_2HPO_4 x $2H_2O$ 15 mM Glucose Adjusted to pH 7.13
Electroporation buffer for THP-1 cells	-	5 mM KCl, 15 mM $MgCl_2$, 15 mM HEPES 50 mM NaCl 150 mM Na_2HPO_4/NaH_2PO_4 pH 7.2
Lysogeny broth-medium	LB-medium	1% (w/v) Bacto-tryptone 0.5 % (w/v) Bacto-yeast extract 1% (w/v) NaCl pH 7.0
Phosphate buffered saline	PBS	137 mM NaCl 2.7 mM KCl 10 mM Na_2HPO_4 1.8 mM K_2HPO_4 adjusted with NaOH to pH 7.4

Phosphate buffered saline with 0.1 % Tween 20	PBS/T	137 mM NaCl 2.7 mM KCl 10 mM Na_2HPO_4 1.8 mM K_2HPO_4 adjusted with NaOH to pH 7.4 + 0.1 % Tween 20
Tris, acetic acid, EDTA buffer	TAE buffer	40 mM Tris 20 mM acetic acid 1 mM EDTA
Tris buffered saline	TBS	150 mM NaCl 50 mM Tris-Cl Adjusted with NaOH to pH 7.4
Tris buffered saline with 0.1 % Tween 20	TBS/T	150 mM NaCl 50 mM Tris-Cl Adjusted with NaOH to pH 7.4 + 0.1 % Tween 20
Tris buffered saline with 0.1 % Tween 20 and 0.01 % SDS	TBS/TS	150 mM NaCl 50 mM Tris-Cl Adjusted with NaOH to pH 7.4 + 0.1 % Tween 20 + 0.01 % SDS
Tris buffered saline with 0.1 % Triton X 100	TBS/X	150 mM NaCl 50 mM Tris-Cl Adjusted with NaOH to pH 7.4 + 0.1 % Triton X 100

2.4 Table 4: Antibodies

Host and antigene	Supplied by	Reference number
Mouse anti RelA	Cell Signaling Technologies, Danvers, Massachusetts, USA	6956
Rabbit anti Ser536 phosphorylated RelA	Cell Signaling Technologies	3033
Rabbit anti Ser32 phosphorylated IκB	Cell Signaling Technologies	9246
Goat anti-Mouse Cy3 conjugated	Thermo Fisher Scientific	A10521
Rabbit anti $p\beta_2$-AR355/356	Santa Cruz Biotechnology, Dallas, Texas, USA	Sc-16719-R
Goat anti-Rabbit IRDye® 800 CW	LI-COR	925-32211

2.5 Table 5: Chemicals

Name	Supplied by	Reference number
α-Hederin	Phytolab, Vestenbergsgreuth, Germany	89220
Corticosterone	Sigma-Aldrich	46148
3,4- Dicaffeoylquinic acid	Phytolab	80425
3,5- Dicaffeoylquinic acid	Phytolab	80426
4,5- Dicaffeoylquinic acid	Phytolab	80427
Hederacoside B	Stanford Chemicals, California, USA	-
Hederacoside C	Phytolab	89221
Hederacoside D	Phytolab	84218
ICI 118,551 hydrochloride	Sigma-Aldrich	I127
Lipopolysaccharide from E. coli	Sigma-Aldrich	L2630
Kaempferol-3-O-rutinoside	Phytolab	80700
Paroxetine hydrochloride hemihydrate	Sigma-Aldrich	P9623
Rutin	Phytolab	89270
Terbutaline hemisulfate	Sigma-Aldrich	T2528
Tumor necrosis factor α	Merck Millipore, Massachusetts, USA	GF314

3 Methods

3.1 Characterization of EA 575® by HPLC analysis

EA 575® (CID-100048) was dissolved in 50 % EtOH in a concentration of 40.8 mg/ml. EA 575® was filtrated through a 0.45 µm PTFE filter and analyzed on a Agilent Series 1200 HPLC system equipped with a degasser (G1322A), a quaternary pump (G1311A), an autosampler (G1329A), and a photodiode array detector (G1315D) using a LiChrospher RP-18 column (5 µm, 125 x 4 mm, Merck, Darmstadt). Solvent A was H_2O/acetonitrile (44/2, m/m) adjusted to pH 2.0 with phosphoric acid 85 %. Solvent B was acetonitrile. The following linear gradient was used: 0-9 min 0 % B, 9-10 min to 6 % B, 10-25 min to 15 % B, 25-50 min to 60 % B, 50-51 min to 100 % B, 51-65 min 100 % B. Flow rate: 0-50 min 1 ml/min, 51-65 min 1.5 ml/min. Detection: 205 nm. Identification of rutin, 3,4-dicaffeoylquinic acid (3,4-DCA), 3,5-dicaffeoylquinic acid (3,5-DCA), 4,5-dicaffeoylquinic acid (4,5-DCA), kaempferol-3-O-rutinoside, hederacoside C, hederacoside D, hederacoside B, and α-hederin was carried out by comparison of UV spectra of reference substances and their corresponding retention times, as shown in supplemental material (Table S 1). α-Hederin amount was quantified by the determination of reference peak area equal to 1 µg α-hederin and the corresponding area in extract analysis. The calculations and a reference chromatogram are shown in supplemental material (Table S 2**,** Table S 3**,** and Figure S 1). The integration parameters were set to a slope sensitivity of 5, a peak width of 0.05, an area reject of 20, an height reject of 1, and shoulders off. The chromatograms were registered and evaluated using Agilent Chemstation Software Version B.04.

3.2 Cell culture

HEK 293 cells, subsequently called HEK cells, were cultivated in DMEM supplemented with 5 ml P/S and 10 % FCS for 500 ml medium. HEK cells and all constructed clones were subcultured 1:10 every 3-4 days in 10 cm cell culture dishes. THP-1 cells were maintained in

a RPMI medium supplemented with 10 % FCS, 5 ml P/S, 50 µM β-mercaptoethanol and 5 ml Glutamax for 500 mL medium. THP-1 cells as well as the Nanoluc-PEST clone were subcultured 1:3 every 2-3 days in 75 cm^2 flasks. J774.2 cells were cultured in a DMEM without phenol red supplemented with 5 ml P/S, 5 ml L-Glutamine and 10 % FCS for 500 ml medium, cells were subcultured 1:10 every 2-3 days in 10 cm plates. All cells were cultured at 37° C with 5 % CO_2.

3.3 Generation of NFκB reporter plasmid

For the generation of a NanoLuciferase with an associated PEST sequence (Nanoluc-PEST) under control of an NFκB binding sequence the pNFκB-D2EGFP vector (Clontech) was used as origin. The destabilized GFP was removed from the vector by PCR, introducing a new XhoI-site (forward primer: 5'TCGGATATCTCGAGCCGGAATTCGGGGAAGCTTC-3'; reverse primer: 5'-GTTCAGGGGGAGGTGTG-3'). The Nanoluc-PEST sequence was cut from pNL1.2[NlucP] vector using BamHI/XhoI and introduced via ligation into the pNFκB vector. Ligation was performed for 1 h at room temperature by combining 1 Unit T4-DNA ligase with 20 ng vector-DNA and 3fold amount of the insert-DNA fragment in 1x ligase buffer. Subsequently, the vector was recaptured from a 1 % agarose gel and amplified in XL1-blue cells as described in chapter 3.5. For analysis the vector was enzymatically digested by BglI and PstI and fragment sizes were matched. The found fragments corresponded to the expected fragment sizes of 4597+1299 for BglI enzymatic digest, and 3155+2741 for PstI enzymatic digest, respectively. The agarose gel of enzymatic digestions and the plasmid card are shown in the supplemental material (Figure S 2, Figure S 3). Integrity of the final construct was additionally confirmed by a cycle sequencing performed by GATC.

3.4 Generation of IκBα-nVenus and RelA-cVenus

The protein fragment complementation (PFC) plasmids, pCDNAHygr_cVenus-RelA and pCDNAZeo_IkBa-nVenus were constructed by GeneArt according to the publication of Yu et al. [8]. For verification, the plasmid pCDNAZeo_IkBa-nVenus was enzymatically digested

with BglI and PstI. The vector showed the expected band sizes in an agarose gel analysis. Also, pCDNAHygr_cVenus-RelA was enzymatically digested with EcoRI and showed the expected band sizes. The agarose gels of digestions and the plasmid cards are shown in the supplemental material (Figure S 4, Figure S 5, Figure S 6, and Figure S 7). The vector was amplified in XL1-blue as described in chapter 3.5. Integrity of the final construct was additionally confirmed by a cycle sequencing performed by GATC.

3.5 Transformation of XL1-blue bacteria cultures

For the amplification of the DNA constructs described above, approximately 1 ng of DNA was mixed with 100 µl competent XL-1 blue bacteria and the mixture was kept on ice for 30 min. A heat shock was performed by heating the mixture for 30 s at 42°C and suddenly cooling it on ice for 1 min.

900 µl of pre-warmed LB medium was added to the bacteria–DNA mix and the mixture was incubated in a shaker at 37°C for 1 h. Afterwards, 100 to 500 µl of the DNA-bacterial cells mixture were spread on agar-LB-medium plates (1.5 % w/v agar in LB-medium) containing the same antibiotic as used for selection and incubated at 37°C overnight. Single clones arising from single bacterial cells were picked and inoculated each in 5 ml LB-medium containing the appropriate antibiotic (50 µg/ml ampicillin or 25 µg/ml kanamycin) and incubated at 37°C overnight in a shaker. The next day 500 µl of pre-culture was added to 25 ml fresh, antibiotic containing LB-medium and allowed to grow for 8 h.

Plasmid DNA was isolated by midi prep isolation kit (Qiagen®) according to the manufacturer's instructions (Figure S 8), digested with the suitable restriction enzymes, and the correct insert size verified by agarose gel electrophoresis in comparison to a DNA standard ladder.

3.6 Agarose gel electrophoresis

An agarose gel (1 %) was prepared by suspending the required amount of agarose in 1 x TAE buffer and heating in a microwave oven until the solution became clear. After cooling the solution down to approximately 55°C, ethidium bromide was added in a final concentration of 1 µg/ml and the mixture was allowed to polymerize in a prepared casting tray with a suitable comb size. After being completely polymerized, the gel was placed into an electrophoresis chamber filled with 1 x TAE buffer. The DNA samples were mixed with the sample buffer and slowly loaded into the wells before an electric current was applied (3-10 V/cm2) for 30 min. Finally, DNA fragments were detected using an UV detector.

3.7 Transfection of HEK cells

HEK cells were transfected by calcium phosphate method. The cells were seeded in 12 well plates and allowed to attach for at least 24 h. Before transfection, the medium was changed to 900 µl fresh, fully supplemented medium. One µg DNA was mixed with 6.5 µl 2 M CaCl2 and 50 µl sterile water. The mixture was added dropwise to 2x HBS pH 7.13 and after half an hour of resting added to the cells. After 24 h the medium was changed to fresh DMEM containing antibiotic for selection. After one week of selection single clone was picked by trypsination in a cloning ring and seeded in a distinct 12 well plate for further growth. For selection of Nanoluc-PEST clones 700 µg/ml geneticin, for IκBα-nVenus clones 150 µg/ml Zeocin and for RelA- cVenus clones 100 µg/ml Hygromycin was used, respectively. The cloning procedure of β_2AR GFP plasmid and its transfection to HEK cells were described previously [3, 9]. HEK β-arrestin 1/2 KO cells were a kind gift of Asuka Inoue (Graduate School of Pharmaceutical Sciences, Tohoku University Japan). Asuko Inoue therefore modified HEK cells by CRISPR/Cas9 genome editing to eliminate β-arrestins (β- arrestin1 and β-arrestin2), as described in the work of Alvarez-Curto et al [10].

3.8 Transfection of THP-1 cells

THP-1 cells were transfected by Amaxa electroporation technology, Nucleofector® II. For each transfection 2x 10^6 cells were diluted in 100 µl of a self-made electroporation buffer with 1 µg DNA and transfected with the program T-020. Afterwards they were transferred to a 12 well plate with 1 ml fresh, fully supplemented RPMI medium. After 24 h the medium was changed to full medium containing 700 µg/ml geneticin for selection. Every 2-3 days the medium was changed by 10 min centrifugation with 90 rcf. After one week of selection the mixed clone grew up.

3.9 In-Cell Western™ measurement for phosphorylated β_2-adrenergic receptor (Ser355/356)

96 well plates were coated with 40 µl of 0.1 mg/ml PDL for 30 min and afterwards washed three times with 50 µl PBS. HEK β_2AR GFP cells were seeded in a fully supplemented growth medium in a density of 15000 cells per well and allowed to grow to a confluency of 80 % and starved overnight in serum-free medium. Pre-incubation with α-hederin was performed for 8 h. Next morning GRK2 inhibition with 10 µM paroxetine was performed for 45 min. The cells were stimulated with 1 µM terbutaline, or 0.5 µM isoprenaline, respectively, in serum-free medium for 20 min. Afterwards the fixation was done with 15 % sucrose 4 % PFA in PBS for 30 min. The permeabilization was performed with TBS/X five times for five min. Cells were blocked for 1 h with Odyssey blocking buffer and afterwards incubated with the primary antibody (rabbit anti pβ_2AR355/356) diluted 1:200 in Odyssey blocking buffer for 2.5 h. The goat-anti-rabbit IRDye800 antibody in a dilution of 1:800 in Odyssey blocking buffer supplemented with 0.05 %Tween 20 was used for the immunostaining. Additionally, the nuclei were stained with Draq5 and Sapphire700 in dilutions of 1:2000 and 1:1000, respectively. Immunostaining was done for 1 h in the dark. After the fixation step, the plate was washed 3 times with TBS/T in between each step. The dried plate was measured on an Odyssey classic reader in 700 and 800 nm channels. Calculation was done dividing data registered at 800 nm channel (phosphorylation) through the appropriate data registered at

700 nm channel (cell number), which is named as near-infrared ratio (NIR ratio), and normalizing it on the terbutaline or isoprenaline stimulated control, respectively.

3.10 Dynamic mass redistribution measurements

For the dynamic mass redistribution measurements, HEK, HEK β_2AR GFP, and HEK β-arrestin 1/2 KO cells were seeded in a density of 6000 cells per well in a 348 well plate (Corning: #5042) and allowed to grow in full growth medium to a confluency of 90 %. For the incubation with ivy leaves dry extract medium was changed to serum-free medium and cells were incubated with 40, 80, or 240 µg/ml EA 575® or 1 µM α-hederin respectively, for 8 h. Afterwards medium was replaced by HBSS buffer supplemented with 20 mM HEPES and the corresponding cells were incubated for 1 h with 10 µM paroxetine or ICI 118551, respectively, both in HBSS buffer supplemented with 20 mM HEPES. The compound plate was prepared with 4-fold concentrations of the used chemicals and loaded into a pipette robot at 37°C. The assay plate was loaded into the Corning® label free Epic® III reader at 37°C and baseline acquisition was done for 300 sec before the stimulation was performed via the pipette robot with 10 µl of the 4-fold solutions of terbutaline or buffer alone. The measurement was recorded for 30 min. Results were documented as changes of the wavelength of the reflected light in pm over time.

3.11 PathHunter® assay with CHO K1 ADRB2 eXpress cells

CHO K1 ADRB2 eXpress cells were thawed and resuspended in 20 ml of the provided CP medium. One hundred µl cell suspension per well was seeded in a white 96 well plate included in the assay kit and allowed to grow for 24 h. The incubation was performed overnight with EA 575® or α-hederin in the indicated concentrations, respectively. Inhibition of GRK2 was done with 10 µM paroxetine for 45 min. Afterwards the cells were stimulated with 1 µM terbutaline for 90 min. The detection of the chemiluminescent signal was carried out according to the manufacturer's instructions (Figure S 11). The bottom side of the plate was

masked with a white non-transparent adhesive foil and the luminescence was measured in a Tecan Genios® plate reader.

3.12 Determination of IL-6 in J774.2 cells

For the IL-6 measurements J774.2 cells were seeded in 12 well plates at a density of 60000 cells per well and were allowed to grow for 24 h. The increased release of IL-6 into the cell supernatant was induced by 10 ng/ml LPS for 12 h. Incubation of cells with 1.7 µg/ml (5 µM) corticosterone together with 10 ng/ml LPS for 12 h was used as a negative control. EA 575® was tested in concentrations of 40, 80 and 160 µg/ml incubated for 12 h simultaneous with LPS. The cell supernatants were used for IL-6 determination with a Novex® mouse IL-6 ELISA kit according to the manufacturer´s instructions provided as supplemental material (Figure S 12). The absorbance was measured on a Tecan Genios® Reader at 450 nm.

3.13 Measurement of NFκB transcriptional activity through a Nanoluc-PEST reporter system in HEK Nanoluc-PEST and HEK β-arrestin 1/2 KO Nanoluc-PEST cells

96 well LumiNunc™ plates were coated with 40 µl of 0.1 mg/ml PDL for 30 min and afterwards washed three times with 50 µl PBS. HEK cells or HEK β-arrestin 1/2 KO cells both stably expressing Nanoluc-PEST were seeded in a density of 15000 cells per well in 100 µl total growth medium and allowed to grow to a confluency of 90 %. The medium was changed to serum-, and antibiotic-free medium. Incubation was performed with 40, 80 or 240 µg/ml EA 575® for 8 h, respectively. For the co-stimulation with terbutaline an incubation time of 8 h and a concentration of 1 µM was considered to be most promising. The best measurement conditions for TNFα were identified through a time- and dose-dependent measurement and were therefore set to a dose of 25 ng/ml and an incubation time of 3 h within the EA 575® and/or terbutaline incubation. (Figure S 14). Measurement of luciferase activity was achieved using the Nano-Glo® Luciferase Assay system as described in chapter 4.A and 4.B of the manual (Figure S 13). The bottom side of the plate was masked with a white non-transparent adhesive foil and luminescence was measured in a Tecan Genios® plate reader.

3.14 Measurement of NFκB transcriptional activity through a Nanoluc-PEST reporter system in THP-1 cells

THP-1 Nanoluc-PEST cells were seeded in 96 well LumiNunc™ plates in a density of 100000 cells/ml and incubated immediately with 40, 80 or 240 µg/ml EA 575® for 8 h, respectively. After 5 h, LPS was added to a concentration of 10 ng/ml for 3 h which was decided upon time- and dose dependent measurements shown in the supplemental material (Figure S 15). The measurement of luciferase activity was performed using the Nano-Glo® Luciferase Assay system as described in chapter 4.A and 4.B of the manual (Figure S 13). The bottom side of the plate was masked with a white non-transparent adhesive foil and luminescence was measured in a Tecan Genios® plate reader.

3.15 Immunolocalization of RelA in HEK cells

Glass coverslips were coated with 0.1 mg/ml PDL for 30 min in 12 well plates and subsequently washed three times with PBS. HEK cells were seeded on the coverslips in a density of 100000 cells per well. At a cell confluency of 90 % medium was changed to plain medium and cells were incubated for 8 h with 240 µg/ml EA 575® or 0.5 % ethanol as a control. After 7 h and 10 min TNFα was added to a concentration of 25 ng/ml for 50 min. Afterwards the cells were fixed with freshly prepared 4 % formaldehyde in PBS, permeabilized with ice-cold methanol for 10 min and blocked with 5 % BSA in PBS supplemented with 0.3 % Triton X-100. The immunostaining was performed with an antibody targeting RelA in a dilution of 1:800 overnight and a Cy3 coupled secondary antibody in a dilution of 1:400 for 1.5 h in the dark. Additionally, cells were incubated with Hoechst 33528 for a nuclear staining. For long-term storage cells were mounted on object slides with ProLong® antifade diamond. In between each step the cells were washed with PBS. After incubation with the secondary antibody the cells were additionally washed with deionized water. Images were taken on a Zeiss Axiovert 200 M with a LCI Plan-Neofluar 63x/1.30 Imm Korr Ph 3 M27 objective using an AxioCamHR.

3.16 Immunolocalization of RelA in J774.2 cells

J774.2 cells were seeded on coverslips in a density of 100000 cells per well. After they reached a confluency of 90 %, the cells were incubated overnight with 80 µg/ml EA 575® or 0.5 % ethanol. The following day cells were stimulated for 60 min with 100 ng/ml LPS. Afterwards the cells were fixed with 4 % formaldehyde in PBS, permeabilized with ice-cold methanol for 10 min and blocked with 5 % BSA in PBS supplemented with 0.3 % Triton X-100 for 1 h. Immunostaining was performed with an antibody targeting RelA in a dilution of 1:800 overnight and a Cy3 coupled secondary antibody in a dilution of 1:400 for 1.5 h in the dark. Additionally, cells were incubated with Hoechst 33528 for a nucleus staining. For long-term storage cells were mounted on object slides with ProLong® antifade diamond. In between each step cells were washed with PBS. After incubation with the secondary antibody the cells were additionally washed with deionized water. Images were taken on a Zeiss Axiovert 200 M with a LCI Plan-Neofluar 63x/1.30 Imm Korr Ph 3 M27 objective using an AxioCamHR.

3.17 Western blot analysis

HEK cells were seeded in 12 well plates and allowed to grow to a confluency of 80-90 % in full-growth medium. The cells were incubated in a plain-medium with 240 µg/ml EA 575® for 8 h and afterwards with 25 ng/ml TNFα for 10 min. After the incubation cells were harvested with 100 µl 10 mM HEPES buffer pH 7.4 per well containing the appropriate amounts of phosphatase inhibitor cocktail and protease inhibitor cocktail. Cell solutions were sonified for 15 sec with 40 kHz and lysed by being forced through a 30 G cannula. To separate cell debris the solution was centrifuged with 15000 rcf for 5 minutes at 4°C. Fifteen µl supernatant was diluted with 5 µl 4x sample buffer NuPAGE® and 20 µl of the samples were separated in a 10 % acrylamide gel with 80 V in the stacking (5 %) and 120 V in the resolving gel. The blotting was done with 200 mA per gel in a semi-dry blotter for 45 min. For normalization the membrane was stained after blotting with REVERT™ total protein stain according to the manufacturer´s instructions supplied in the supplemental material (Figure S

19). The intensity was measured on a LI-COR Odyssey classic reader in 700 nm channel. Afterwards the stain was removed as described in the manual and the membrane was blocked with Odyssey blocking buffer (TBS) for 1 h. Detection of the phosphorylated proteins was performed by incubating the membrane in Odyssey blocking buffer diluted 1:1 with TBS/T containing the respective antibodies against phosphorylated IκBα or phosphorylated RelA in a dilution of 1:1000. After washing three times in TBS/T the membrane was incubated with secondary antibody (LI-COR Goat anti Rabbit IRDye800, 1:10000) in Odyssey blocking buffer diluted 1:1 with TBS/TS for 1 h. Membrane was washed three times in TBS and measured again on a LI-COR Odyssey classic Reader in 800 nm channel. The normalized protein concentration was received by dividing the signal intensity value of the phosphorylated protein by the respective normalization factor of REVERT™ total protein stain.

3.18 Protein fragment complementation assay

Black 96 well plates (CellCarrier™) were coated for 30 min with 0.1 mg/ml PDL in PBS. Residual PDL was removed by three washing steps with PBS. HEK cells stably expressing IκBα-nVenus and RelA-cVenus were seeded into these plates in total growth medium and allowed to grow to a confluency of 90 %. After reaching confluency the cells were pre-incubated for 8 h with the indicated concentration of EA 575® in HBSS buffer supplemented with 20 mM HEPES. Terbutaline incubation was performed for 2 h in concentrations of 0.1, 1 and 10 µM, respectively. After pre-incubation the cells were stimulated with 10 ng/ml TNFα and the decrease of fluorescence intensity was measured for 3 h in a Perkin Elmer EnSight reader with excitation at 515 nm and emission at 550 nm and normalized through the cell density determined by transmission pictures and analysis by Kaleido™ 2.0 software.

3.19 Statistical data evaluation

Statistical data evaluation was performed with One-way ANOVA followed by Tukey multiple comparison test. Results were considered to be significant for p-values < 0.05.

4 Results

4.1 HPLC fingerprint analysis of EA 575®

The used batch of EA 575® was analyzed by the described HPLC method. Rutin, 3,4-DCA, 3,5-DCA, 4,5-DCA, kaempferol-3-O-rutinoside, hederacoside C, hederacoside D, hederacoside B, and α-hederin were identified in the HPLC chromatogram by comparison of both the retention time and the UV spectra of their corresponding reference substances. A table of the retention times of the identified EA 575® ingredients can be found in the supplemental material (Table S 1). α-Hederin was additionally quantified through the determination of the peak area in relation to the peak area corresponding to 1 µg of its reference substance. Calculation can be found in the supplemental material (Table S 3). The used extract concentrations are thereby adjusted to the contained α-hederin amount. 80 µg/ml EA 575® correspond to 1 µM α-hederin.

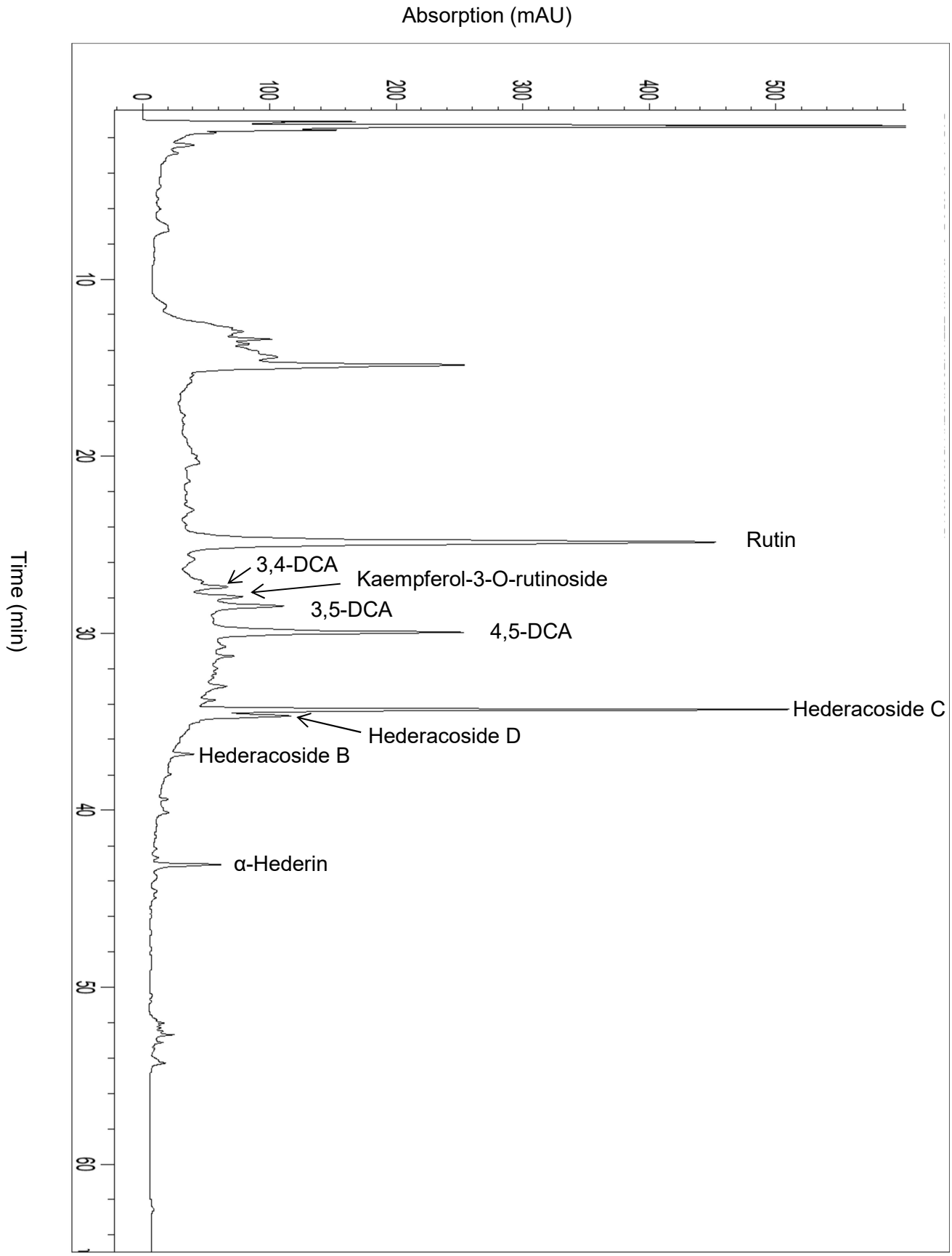

Figure 1: HPLC chromatogram of EA 575®

4.2 Inhibition of β_2-adrenergic receptor phosphorylation at Ser355/356 by α-hederin

As already published, it could be shown that α-hederin, a compound of the ivy leaves dry extract EA 575®, is able to inhibit the GRK2 mediated phosphorylation of β_2AR [11]. For this study HEK β_2AR GFP cells were stimulated with isoprenaline. Phosphorylation was measured in an In-Cell Western™ assay with a Ser355/356 phosphorylation specific antibody. α-Hederin dose-dependently decreased the isoprenaline induced β_2AR phosphorylation at Ser355/356. A concentration of 0.5 µM α-hederin inhibited the phosphorylation by 17.0 %, while 1 µM α-hederin even reduced it by 20.4 % (Figure 2).

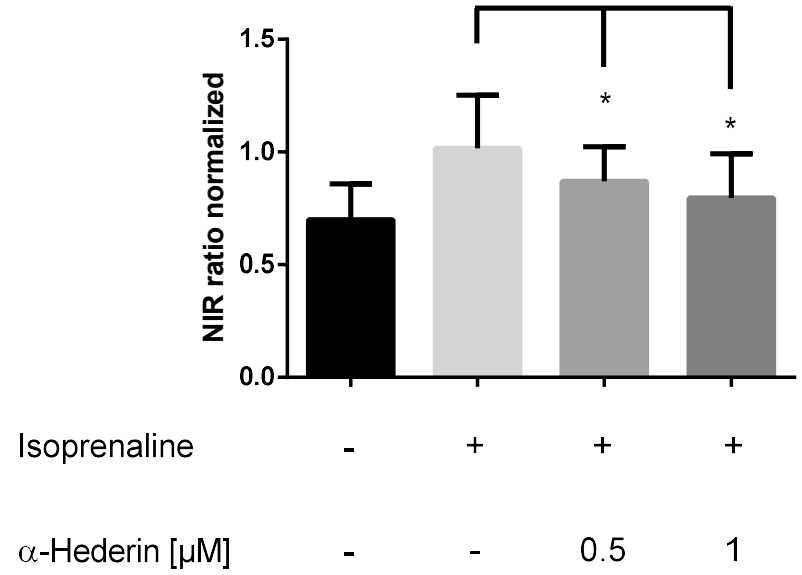

Figure 2: Phosphorylation of the β_2AR at Ser355/356 measured in HEK β_2AR GFP cells after 8h pre-incubation with the indicated amounts of α-hederin and stimulation with 0.5 µM isoprenaline for additional 20 min. The presented data was generated in cooperation with Anne Wolf. Data represent the mean and S.D. of at least three independent experiments ($n \geq 30$, $^*p < 0.05$).

4.3 Inhibition of β_2-adrenergic receptor phosphorylation at Ser355/356 by paroxetine

The study previously referred to, used methyl-5-[2-(5-nitro2-furyl)vinyl]-2-furoate as a GRK2 inhibitor according to the publication of Iino et al. [12]. Later on, paroxetine was identified as a GRK2 inhibitor with a lower IC50 value and selectivity for GRK2 over e.g. GRK1 or GRK5, respectively [13]. Therefore in this work paroxetine was used as a GRK2 inhibitor. Usability was shown in an In-Cell Western™ assay by measuring phosphorylation of β_2AR at Ser355/356 after terbutaline stimulation.

Paroxetine was shown to inhibit the terbutaline induced and GRK2 mediated β_2AR phosphorylation dose-dependently by 17.0, 24.4, and 32.0 %, respectively, in concentrations between 1 and 10 µM (Figure 3).

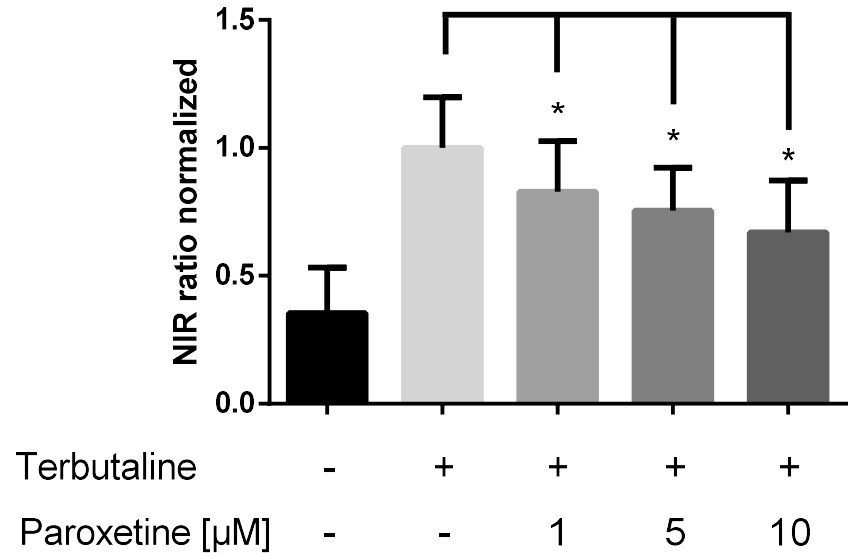

Figure 3: Phosphorylation of the β_2AR at Ser355/356 measured in HEK β_2AR GFP cells after 45 min pre-incubation with the indicated amounts of GRK2 inhibitor paroxetine and stimulation with 1 µM terbutaline for additional 20 min. Data represent the mean and S.D. of at least three independent experiments. ($n \geq 27$, $^*p < 0.05$)

4.4 Dynamic mass redistribution assay

Dynamic mass redistribution assays were established as a high throughput screening for several GPCRs [14]. Stimulation with an appropriate agonist induces a change in the reflected wavelength which can be measured. Terbutaline led to a dose- dependent positive wavelength shift in concentrations between 0.1 nM and 10 µM.

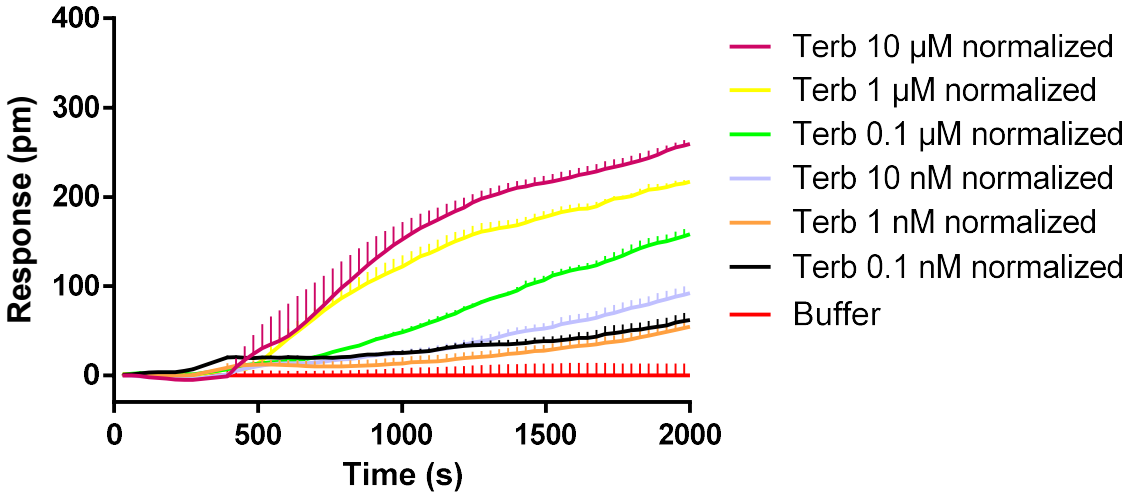

Figure 4: Dose-response of 0.1 nM to 10 µM terbutaline in dynamic mass redistribution measurements in HEK β_2AR GFP cells. Shown is a representative experiment.

The induced positive wavelength shift by 1 µM terbutaline was enhanced by pre-incubation with paroxetine, α-hederin, and EA 575®. Pre-incubation with ICI 118,551 almost completely abolished the terbutaline induced wavelength shift (Figure 5).

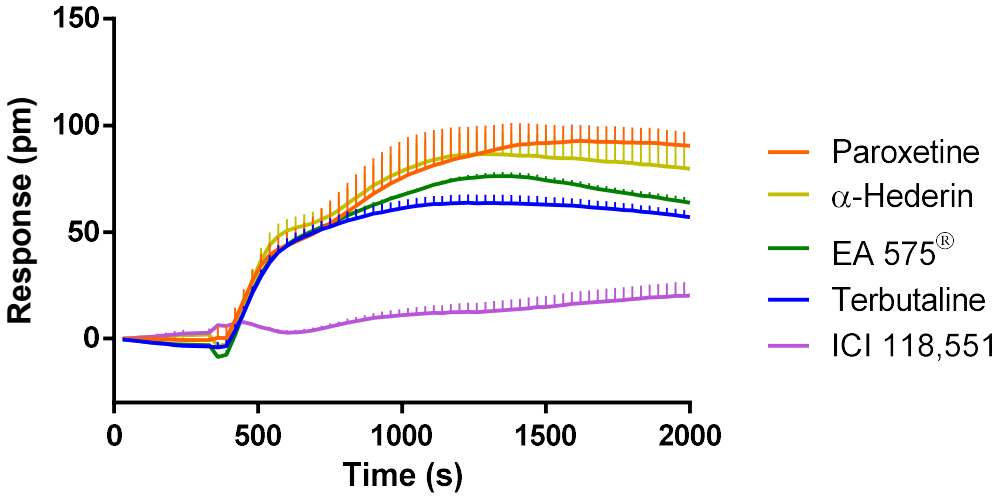

Figure 5: Dynamic mass redistribution measurements in HEK cells after pre-incubation with 10 µM paroxetine or ICI 118,551 for 1 h, or with 1 µM α-hederin or 80 µg/ml EA 575®, respectively, for 8 h prior to stimulation with 1 µM terbutaline after 300 sec of baseline measurements. Measurements are representative for three independent experiments.

To check whether or not β-arrestins are involved in the altered wavelength shift mediated by α-hederin, paroxetine, and EA 575®, respectively, the experiment was repeated with HEK β-arrestin 1/2 KO cells

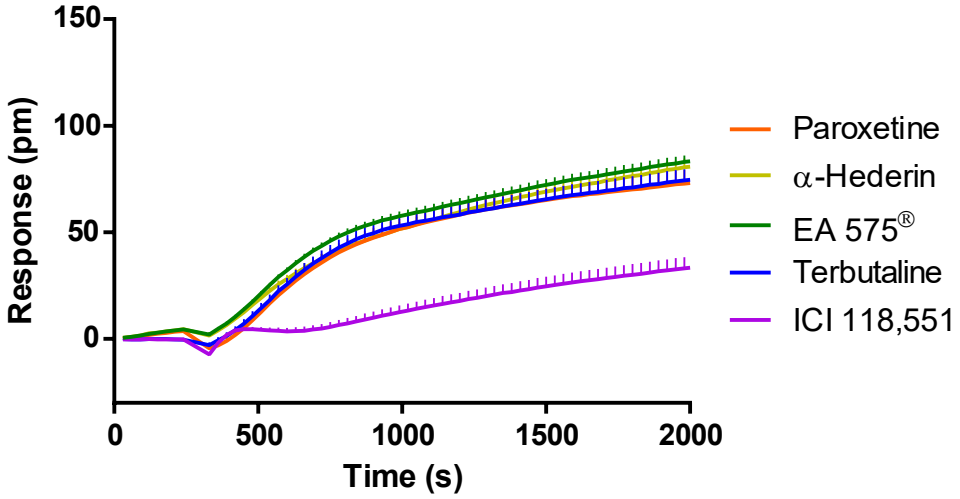

Figure 6: Dynamic mass redistribution measurements in HEK β-arrestin 1/2 KO cells after pre-incubation with 10 µM paroxetine or ICI 118,551 for 1 h, or with 1 µM α-hederin or 80 µg/ml EA 575®, respectively, for 8 h prior to stimulation with 1µM terbutaline after 300 sec of baseline measurements. Measurements are representative for three independent experiments.

In HEK β-arrestin 1/2 KO cells the terbutaline induced wavelength shift was not altered by pre-incubation with paroxetine, α-hederin, or EA 575®, respectively. Thus, the altered wavelength shift under stimulating conditions appears to be β-arrestin dependent. Similar to HEK cells the wavelength shift induced by terbutaline was abolished by pre-incubation with ICI 118,551 (Figure 6).

4.5 PathHunter® assay for β-arrestin 2 recruitment

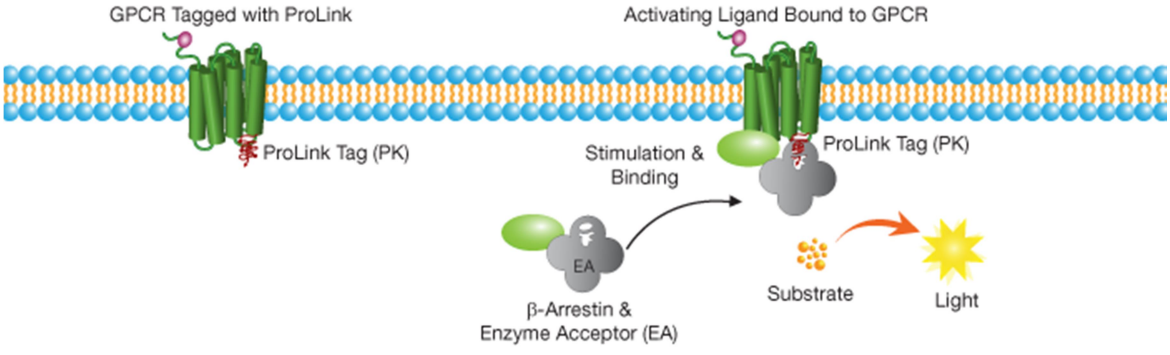

Figure 7: Principle of the PathHunter® β-arrestin 2 assay. Illustration taken from [7].

The GRK2 phosphorylation of β_2AR is known to induce β-arrestin 2 recruitment and thereby trigger the internalization of the receptor [15]. Thus, GRK2 inhibition by α-hederin should also have an impact on the recruitment of β-arrestin 2.

This was investigated by the above shown PathHunter ® β-arrestin 2 assay (Figure 7). Recruitment of β-arrestin 2 was induced by the stimulation with 0.5 µM terbutaline and almost totally inhibited by pre-incubation with the GRK2 inhibitor paroxetine. EA 575® showed a dose-depended decrease in β-arrestin 2 recruitment by 10.7, 20.2, and 26.3 %, respectively, in concentrations between 40 and 240 µg/ml. A pre-incubation with 1 µM α-hederin also led to a reduced recruitment of β-arrestin 2 by 24.3 % (Figure 8).

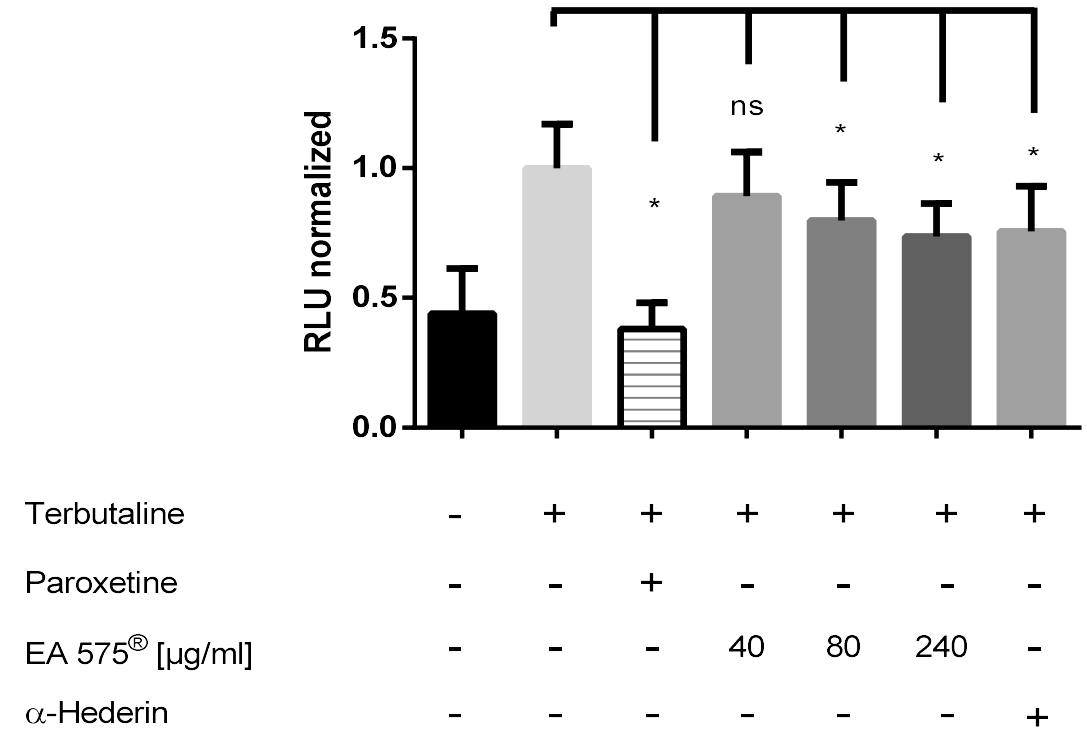

Figure 8: Recruitment of β-arrestin 2 to the β_2AR. Cells were pre-incubated for 45 min with 10 µM paroxetine or overnight with the indicated amounts of EA 575® and α-hederin, respectively, before stimulation with 0.5 µM terbutaline for additional 1h. Data represent the mean and S.D. of at least three independent experiments. (n≥14, ns: not significant, *$p < 0.05$)

4.6 EA 575® decreases IL-6 secretion from murine macrophages (J774.2) after LPS stimulation

To initially check for a possible anti-inflammatory effect of EA 575® the murine macrophage cell line J774.2 was stimulated with 10 ng/ml LPS and the influence of extract pre-incubation on IL-6 secretion was measured by ELISA. As control, J774.2 cells were incubated with 5 µM corticosterone which inhibited the IL-6 secretion by 46.2 %. EA 575® was able to inhibit IL-6 secretion dose-dependently in a concentration range from 40 to 160 µg/ml. The highest concentration of 160 µg/ml EA 575® inhibited IL-6 secretion significantly by 31.6 %, 80 µg/ml EA 575® by 25.4 % (Figure 9).

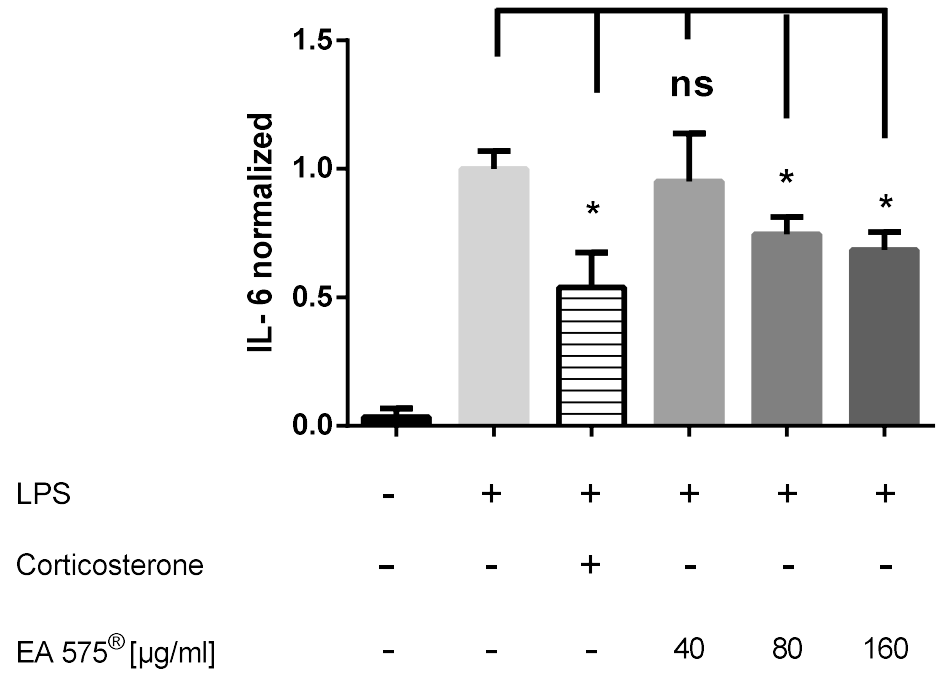

Figure 9: Influence of EA 575® on the IL-6 secretion from J.774.2 cells induced by 10 ng/ml LPS. Corticosterone (5 µM) was used as control. Data represent the mean and S.D. of at least three independent experiments. (n≥8, ns: not significant, * $p<0.05$.)

4.7 Influence of EA 575® on NFκB transcriptional activity after TNFα stimulation

As reported previously, luciferases under the control of NFκB response elements are suitable to verify influences on NFκB transcriptional activity [16]. Therefore HEK cells as well as THP-1 cells were transfected with a Nanoluc-PEST based NFκB reporter system and NFκB transcriptional activity after LPS and TNFα stimulation was monitored. First HEK Nanoluc-PEST cells were stimulated with 25 ng/ml TNFα and within this experiment a dose-depended decrease in NFκB activity after pre-incubation with 40, 80 or 240 µg/ml EA 575® by 31.0, 34.3, and 42.0 %, respectively, was found (Figure 10).

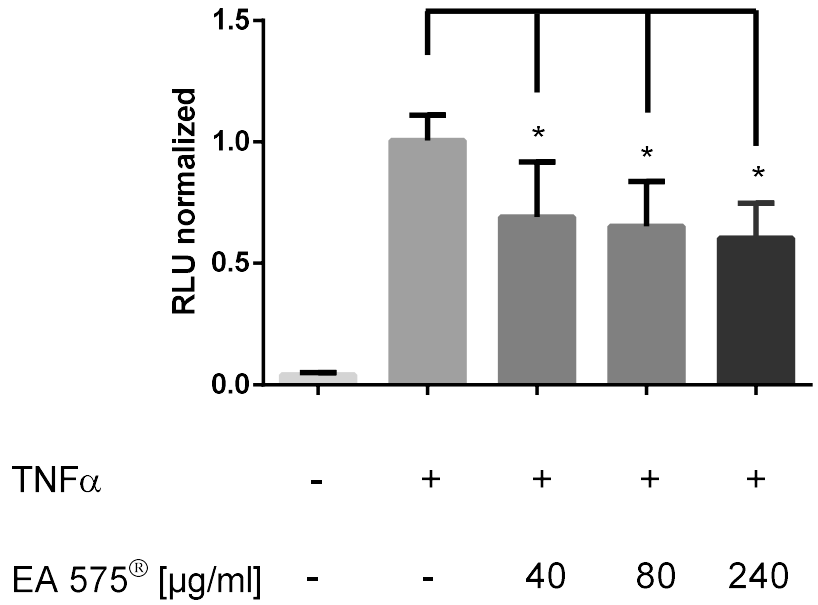

Figure 10: Transcriptional activity of NFκB in HEK Nanoluc-PEST cells after pre-treatment with the indicated amounts of EA 575® for 8h. After 5 h of pre-treatment, cells were stimulated for further 3 h with 25 ng/ml TNFα. Data represent the mean and S.D. of at least three independent experiments. (n≥30, * p<0.05)

Bacteria are recognized by the immune systems through the TLR receptors. In experimental approaches bacterial infections are mimicked with LPS which is recognized by TLR4. As HEK cells do not express TLR4, THP-1 cells were transfected with the Nanoluc-PEST construct and stimulated with 10 ng/ml LPS. Pre-incubation with EA 575® in concentrations between 40 and 240 µg/ml also showed a dose-dependent drop in NFκB activity by 5.8, 12.1, and 25.4 %, respectively, which were significant for concentrations of 80 and 240 µg/ml (Figure 11).

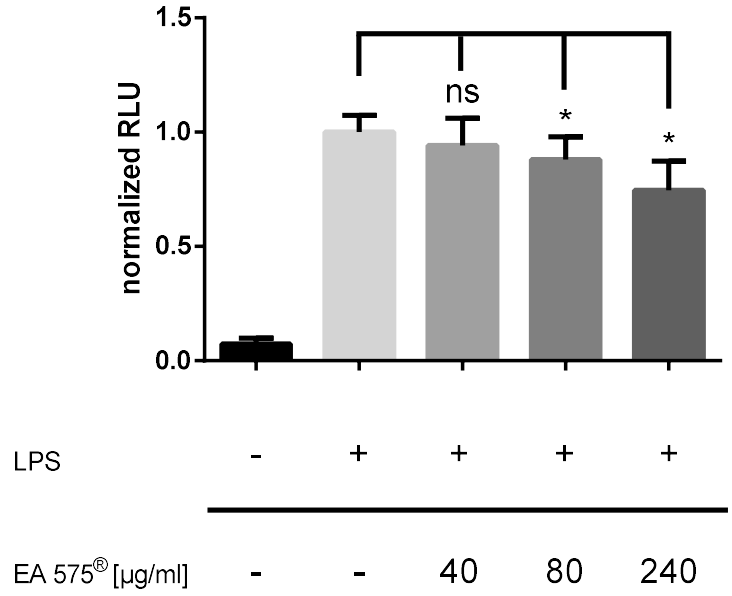

Figure 11: NFκB activity in THP-1 Nanoluc-PEST cells after pre-treatment with different concentrations of EA 575® for 8h. After 5 h of pre-treatment, cells were stimulated for further 3 h with 10 ng/ml LPS. Data represent the mean and S.D. of at least three independent experiments. (n≥24, ns: not significant, *p < 0.05)

4.8 Translocation of NFκB into the nucleus

NFκB transcriptional activity requires the translocation of NFκB into the nucleus. To check whether the decreased transcriptional activity is due to an impaired NFκB translocation an immunofluorescent staining against NFκB subunit RelA in HEK 293 and J774.2 cells was performed. In both cell lines translocation of RelA after stimulation with TNFα or LPS is less pronounced when cells were pre-incubated with different concentrations of EA 575®. The effect was more obvious in J774.2 cells (Figure 12).

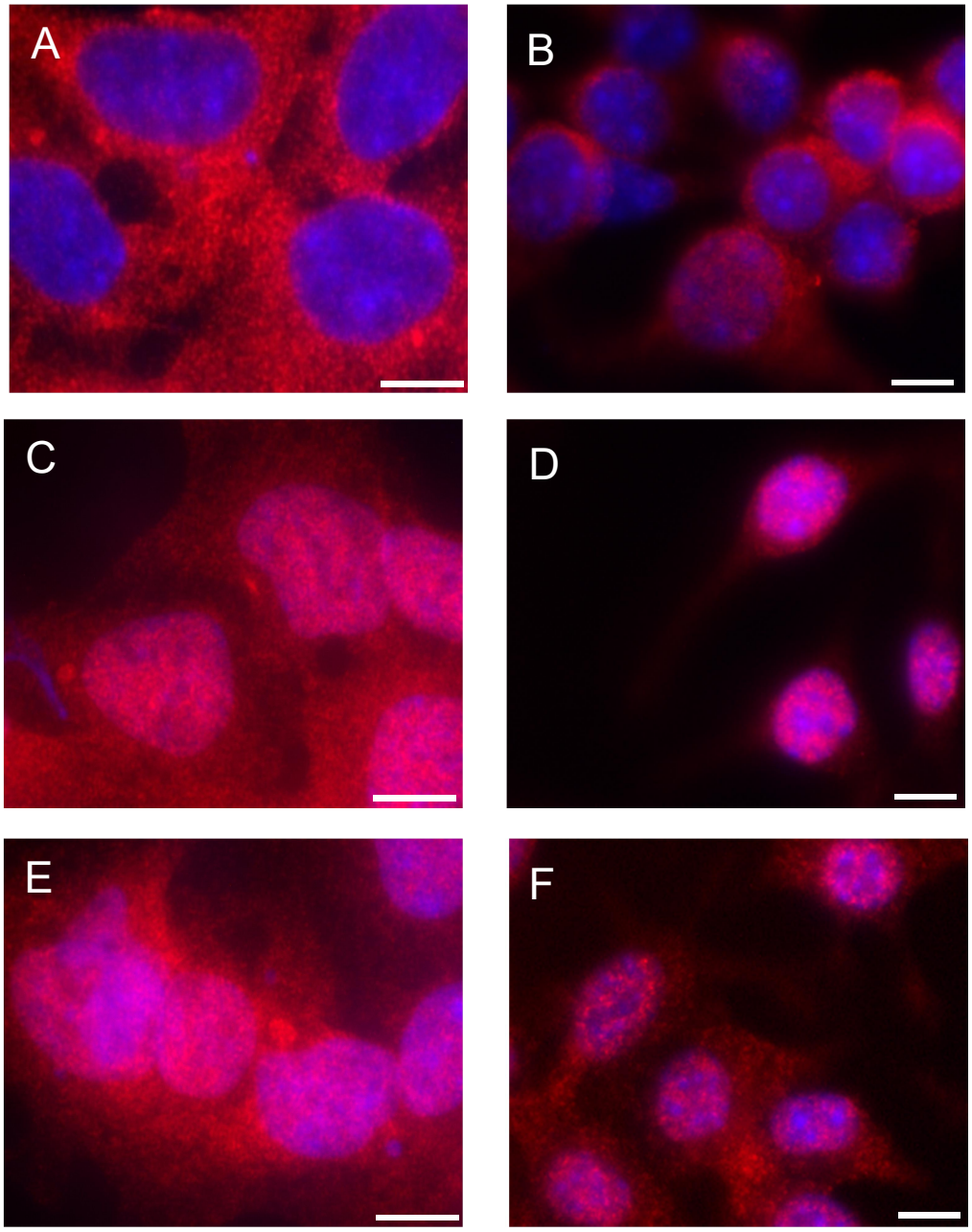

Figure 12: Translocation of NFκB subunit RelA into the nucleus visualized by immunostaining with a primary antibody against RelA and a secondary Cy3 coupled antibody. HEK cells A) unstimulated, C) stimulated with 25ng/ml TNFα for 50 min, E) pre-incubated for 8 h with 240 µg/ml EA 575® and stimulated with 25 ng/ml TNFα for 50 min. J774.2 cells B) unstimulated, D) stimulated with 100 ng/ml LPS for 60 min, F) pre-incubated for 8 h with 80 µg/ml EA 575® and stimulated with 100 ng/ml LPS for 60 min. The nuclei are stained with Hoechst 33528. The scale bars correspond to 10 µM. Pictures are representative for three independent experiments.

4.9 Western blot against phosphorylated IκBα and RelA

IκBα needs to be phosphorylated at Ser32 to dissociate from NFκB which allows NFκB to translocate into the nucleus [17]. The influence of EA 575® on this phosphorylation was investigated by a western blot analysis. HEK cells stimulated with 25 ng/ml TNFα for 10 min revealed an increased phosphorylation of IκBα. Pre-incubation with 240 µg/ml EA 575® significantly lowered the TNFα-induced IκBα phosphorylation by 26.4 % (Figure 13).

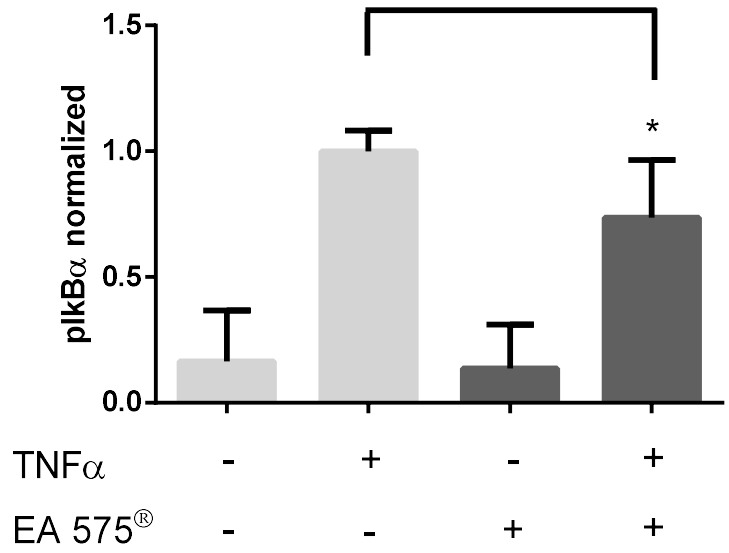

Figure 13: Western blot analysis of phosphorylated IκBα (pIκBα) in HEK cells with or without pre-treatment with 240 µg/ml EA 575® and stimulation with 25 ng/ml TNFα for additional 10 min. Data represent the mean and S.D. of at least three independent experiments. (n≥8, *p < 0.05)

IKKβ is accountable for phosphorylation of IκBα at Ser32 as well as for the phosphorylation of RelA at Ser536 [18]. The influence of EA 575® on RelA phosphorylation was also investigated by a western blot analysis. HEK cells pre-treated with 240 µg/ml EA 575® and subsequently stimulated with 25 ng/ml TNFα revealed an increased formation of phosphorylated RelA (pRelA), which reached a statistically significant level 10 min (Figure 14).

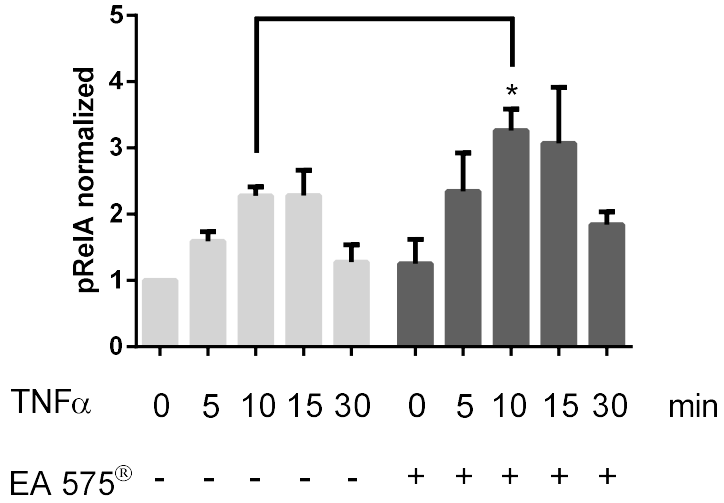

Figure 14: Western blot analysis of phosphorylated RelA (pRelA) in HEK cells with or without pre-treatment with 240 µg/ml EA 575® for 8 h and stimulation with 25 ng/ml TNFα for the indicated time. Data represent the mean and S.D. of at least three independent experiments. ($n \geq 3$, $^*p < 0.05$)

4.10 Protein fragment complementation assay with RelA-cVenus and IκBα-nVenus

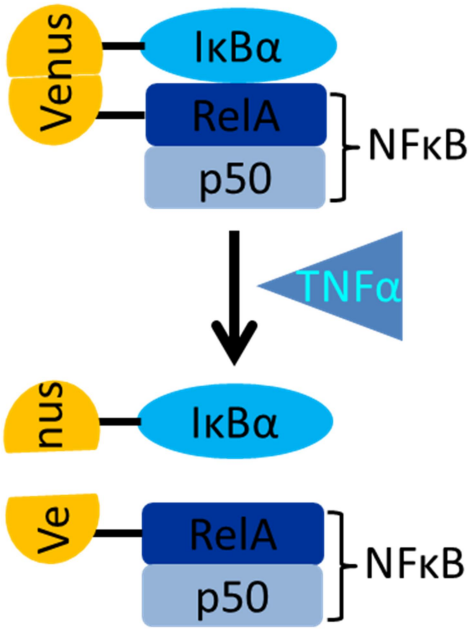

Figure 15: Principle of the protein fragment complementation measurements. Via a plasmid transfection two constructs were introduced into HEK cells. One composed of RelA with the C-terminus of Venus (RelA-cVenus) and the other one of IκBα with the N-terminus of Venus (IκBα-nVenus). Prior to stimulation NFκB and IκBα are complexed and venus is composed of its two halves. Therefore, a fluorescence can be measured at 550 nm (Excitation at 515 nm). After stimulation with TNFα the NFκB:IκBα complex dissociates which decreases the fluorescence intensity.

Phosphorylation of IκBα at Ser32 is known to influence the stability of NFκB:IκBα complexes. Therefore, the dissociation of the complex was determined via a protein fragment complementation of IκBα tagged with nVenus and NFκB subunit RelA tagged with cVenus (Figure 15).

Stimulation of HEK cells stably expressing RelA-cVenus and IκBα-nVenus with 10 ng/ml TNFα led to the disintegration of the complex which can be measured by a drop in fluorescence intensity at 550 nm (Excitation at 515 nm).

Pre-incubation with 160 µg/ml EA 575® for 8 h led to a significant increase of the RelA:IκBα-Venus complex stability under TNFα stimulating conditions. After 3 h of TNFα stimulation 13.9 % more fluorescence was preserved with EA 575® pre-treatment compared to TNFα stimulation alone. Lower concentrations of EA 575® didn´t significantly influence the IκBα:NFκB complex stability (Figure 16).

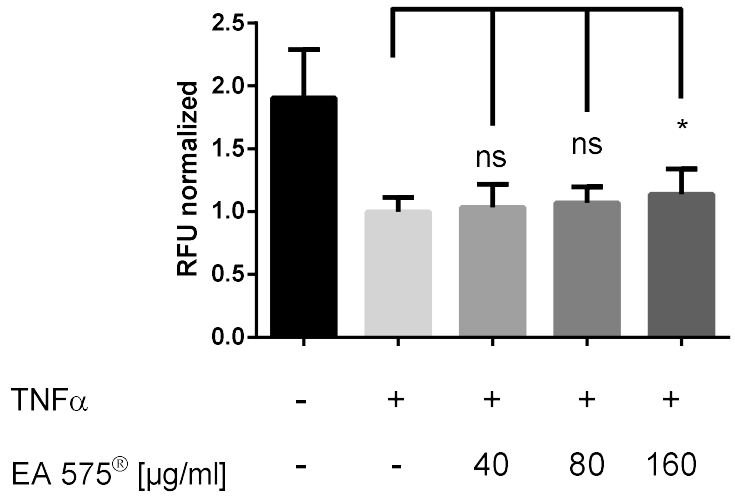

Figure 16: Dissociation of the RelA:IκBα-Venus complex measured by a protein fragment complementation with or without pre-treatment for 8 h with the indicated amounts of EA 575® and after TNFα stimulation for additional 3 h. Data represent the mean and S.D. of at least three independent experiments. (n≥20, ns: not significant, *p < 0.05)

4.11 Influence of β_2-adrenergic receptor stimulation on NFκB transcriptional activity

As reported previously there is a pronounced influence of β_2-adrenergic signaling on inflammatory processes [19-21].

To find out whether the observed influence of EA 575® on the β_2-adrenergic signaling also contributes to its anti-inflammatory effect, the NFκB activity was measured under co-stimulation with 1 µM terbutaline. Stimulation with 1 µM terbutaline for 8 h led to a significant decrease of the TNFα-induced NFκB transcriptional activity by 24.6 % (Figure 17). Like shown before, pre-incubation with EA 575® for 8 h also lowered the TNFα-induced NFκB transcriptional activity in a dose-dependent manner (Figure 17). The simultaneous treatment with EA 575® and terbutaline for 8 h had a synergistic inhibiting effect on TNFα-induced NFκB transcriptional activity by 41.4, 47.0, and 58.5 % with 40, 80 and 240 µg/ml EA 575®, respectively (Figure 17).

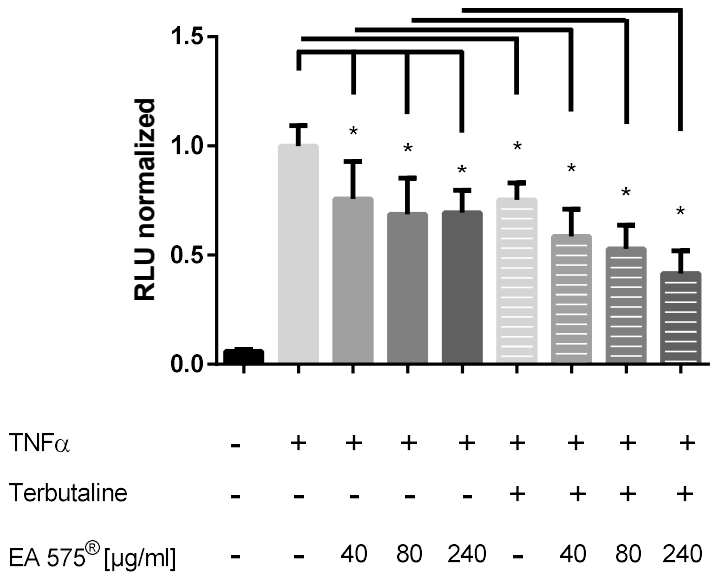

Figure 17: NFκB transcriptional activity in HEK Nanoluc-PEST cells pre-incubated with the indicated amounts of EA 575® for 8 h, co-stimulated with 1 µM terbutaline for 8 h. After 5 h of pre-treatment, cells were stimulated for further 3 h with 25 ng/ml TNFα. Data represent the mean and S.D. of at least three independent experiments. (n≥12, *p < 0.05)

β-Arrestins are thought to be involved in the β_2-adrenergic impact on inflammatory processes [22]. The influence of β-arrestins on the TNFα-induced NFκB transcriptional activity under terbutaline-stimulating conditions was investigated using HEK β-arrestin 1/2 KO Nanoluc-PEST cells. In these cells the effect of EA 575® was less pronounced than in HEK Nanoluc-PEST cells (Figure 18). Dose-dependent inhibition was first significant at a concentration of 80 µg/ml EA 575®, compared to 40 µg/ml EA 575® in HEK cells expressing β-arrestins. Terbutaline was not able to inhibit the NFκB transcriptional activity in HEK β-arrestin 1/2 KO Nanoluc-PEST cells. Equally the synergistic inhibitory effect of EA 575® and terbutaline, observed in HEK Nanoluc-PEST cells, was abolished in HEK β-arrestin 1/2 KO Nanoluc-PEST cells.

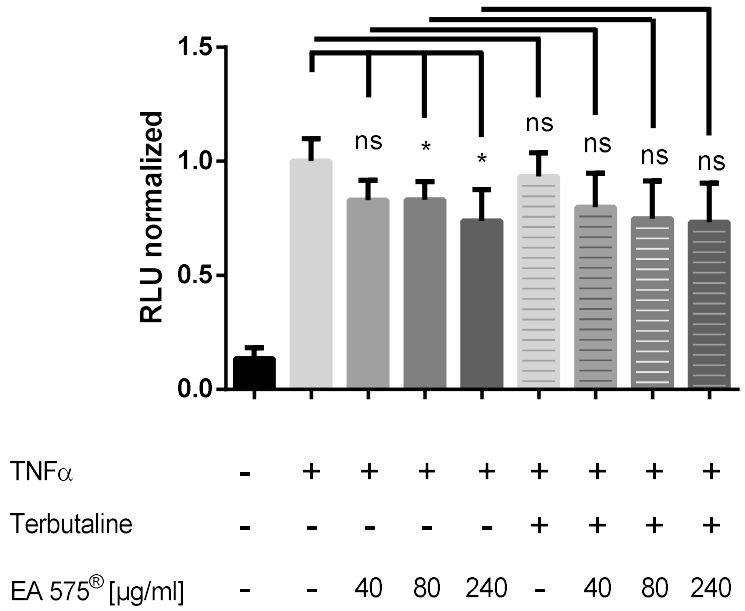

Figure 18: NFκB transcriptional activity in HEK β-arrestin 1/2 KO Nanoluc-PEST cells pre-incubated with the indicated amounts of EA 575® for 8 h, co-stimulated with 1 µM terbutaline for 8 h. After 5 h of pre-treatment, cells were stimulated for further 3 h with 25 ng/ml TNFα. Data represent the mean and S.D. of at least three independent experiments. (n≥12, ns: not significant, *p < 0.05)

4.12 Stabilization of NFκB:IκBα complex under β_2-adrenergic stimulating conditions

A requirement for the transcriptional activity of NFκB is the release of NFκB from the complex with IκBα [23]. Using the protein fragment complementation assay the influence of terbutaline on the RelA:IκBα-Venus complex stability was investigated.

Pre-incubation with terbutaline in concentrations between 0.1 and 10 µM were able to dose-dependently stabilize the RelA:IκBα-Venus complex under TNFα stimulating conditions. This effect was significant for 1 µM and 10 µM terbutaline, stabilizing the complex by 13.4 % and 13.8 %, respectively (Figure 19).

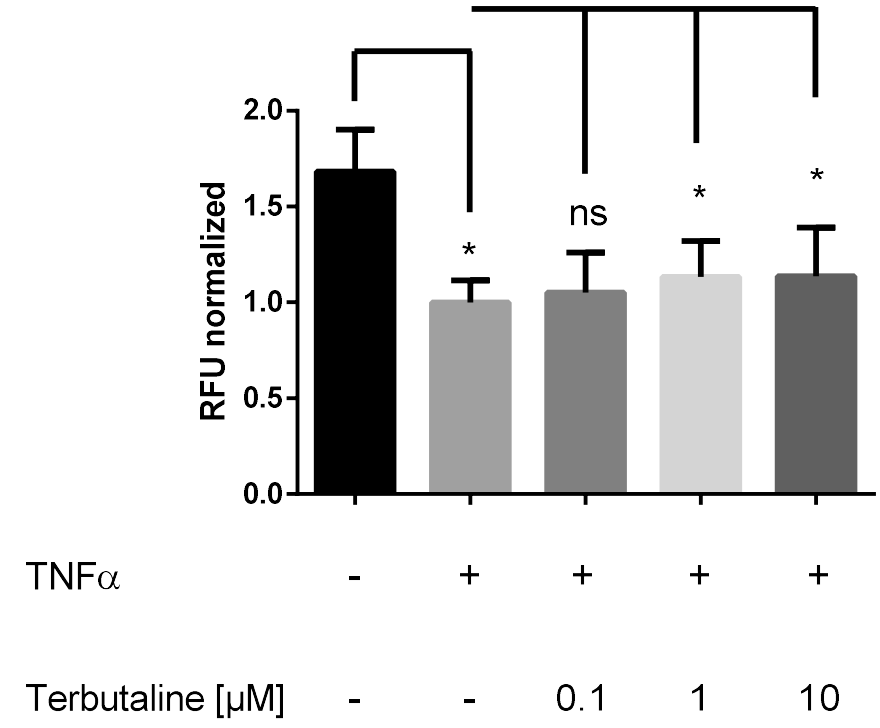

Figure 19: Dissociation of RelA:IκBα-Venus complex measured by the protein fragment complementation in HEK cells pre-treated for 2 h with the indicated amounts of terbutaline and stimulated for additional 3 h with 10 ng/ml TNFα. Data represent the mean and S.D. of at least three independent experiments. (n≥40, ns: not significant, *p < 0.05)

In order to find out whether the NFκB:IκBα complex stabilizing effect of terbutaline is dependent on β-arrestins, the effect was tested on HEK β-arrestin 1/2 KO cells. Again it was found that terbutaline stabilizes the RelA:IκBα-Venus complex in a dose- dependent manner by 15.3 % with 1 µM terbutaline and by 17.9 % with 10 µM terbutaline (Figure 20). Thus, the stabilization of the RelA:IκBα-Venus complex appears to be β-arrestin independent.

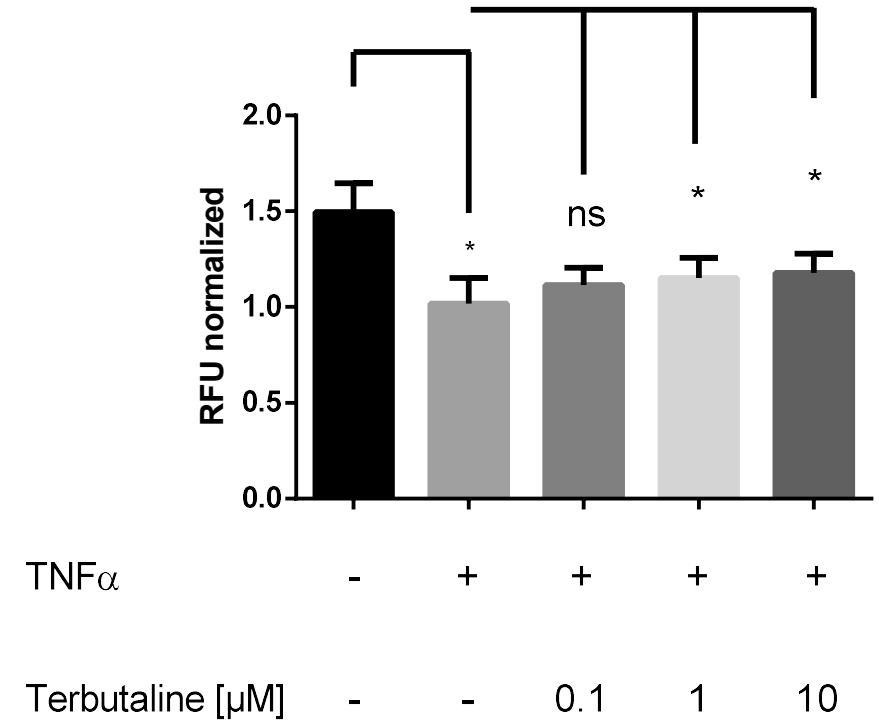

Figure 20: Dissociation of RelA:IκBα-Venus complex measured by protein fragment complementation in HEK β-arrestin 1/2 KO cells pre-treated for 2 h with the indicated amounts of terbutaline and stimulated for additional 3 h with 10 ng/ml TNFα. Data represent the mean and S.D. of at least three independent experiments. (n≥12, ns: not significant, *p < 0.05)

5 Discussion

The ivy leaves dry extract EA 575® is well established for the improvement of symptoms in chronic-inflammatory bronchial diseases and in acute inflammations of the respiratory tract associated with cough.

To characterize the ivy leaves dry extract used in this work, the ingredients hederacoside B, C, D, α-hederin, rutin, kaempferol-3-O-rutinoside, 3,4-, 3,5-, and 4,5-dicaffeoylquinic acid were detected by HPLC fingerprint analysis. Additionally, the amount of α-hederin was determined to adjust the extract concentrations to the appropriate α-hederin concentrations of 0.5 µM, 1 µM and 3 µM which cover the dynamic range of the extract suitable for cell experiments.

The bronchospasmolytic and secretolytic effect of EA 575® seem to derive from the inhibition of β_2AR internalization [3]. This process is initialised by a receptor phosphorylation through GRK2 after stimulation [24]. For α-hederin, considered to be one of the pharmacologically active compounds of EA 575®, it could be shown that the inhibited β_2AR internalization under stimulating conditions is mediated by an indirect inhibition of GRK2 [11]. This leads to a reduced phosphorylation of β_2AR at Ser355/356 (Figure 2). Inhibition of the β_2AR phosphorylation at Ser355/356 by the direct GRK2 inhibitor paroxetine (Figure 3) was also shown to inhibit the receptor internalization [25].

Dynamic mass redistribution (DMR) is a label-free technique to examine signaling events in living cells. In this technique, the wavelength of reflected light changes depending on the optical density of the cells in the adjacent area above the sensor. The optical density of cells changes upon stimulation with appropriate signaling molecules, like terbutaline for β_2AR [26]. Special focus of DMR rests on the signaling pathway of GPCRs, like the β_2AR. Therefore, DMR was chosen to compare the influence of α-hederin and EA 575® on the β_2AR signaling pathway, to that of the direct GRK2 inhibitor paroxetine. Terbutaline induced a dose-dependent positive wavelength shift (Figure 4). Thus, stronger stimulation of β_2AR led to a higher wavelength shift. Inhibition of GRK2, either with α-hederin or EA 575®, or with its direct

inhibitor paroxetine altered the terbutaline-induced wavelength shift (Figure 5) like heightened doses of terbutaline did. The terbutaline-induced wavelength shift was specifically mediated by the β_2AR, as pre-treatment with the antagonist ICI 118,551 almost completely abolished the positive wavelength shift (Figure 5).

DMR functionality was further controlled by stimulation with the muscarinic M2 agonist carbachol and the prostaglandin receptor agonist PGE1 (Figure S 10). Interestingly, an impact of α-hederin on carbachol and PGE1 induced wavelength shift was not observed.

It has been demonstrated that GRK2 mediated phosphorylation of β_2AR is followed by recruitment of β-arrestins to β_2AR to continue with the internalization process. To elucidate whether or not the observed effect of α-hederin, EA 575®, and paroxetine depends on β-arrestins, the measurements were repeated in β-arrestin knock out (KO) cells. As shown in Figure 6 the terbutaline induced wavelength shift could not be altered by pre-incubation with paroxetine, α-hederin, or EA 575®, respectively, in β-arrestin KO cells. It seems, however, as if the altered wavelength shift is associated with an inhibition of β-arrestin dependent receptor internalization.

To further verify the impact of EA 575® on β-arrestin 2 dependent β_2AR signaling, β-arrestin 2 recruitment was measured in a PathHunter® assay. Within this assay α-hederin exhibited an inhibitory effect on β-arrestin 2 recruitment under stimulating conditions. Similarly effective as α-hederin, EA575® reduces β-arrestin 2 recruitment, indicating that there are no synergistic or opposite effects arriving from other extract ingredients (Figure 8).

Glycyrrhizin, structural related to α-hederin, shows widely similar influences on the β_2AR pathway, like inhibition of both GRK2 mediated phosphorylation and receptor internalization [27]. The authors of [27] speculated about a membrane associated effect mostly because of the amphiphilic structure which shares glycyrrhizin with α-hederin. Remarkably, in giant unilamellar vesicles α-hederin forms complexes with cholesterol [28]. Membrane changes like cholesterol depletion were demonstrated to greatly impact clathrin-mediated endocytosis

[29, 30]. The β_2AR is also internalized via clathrin-coated pits and it was additionally shown that downstream signaling of the receptor is highly influenced by changes in the membrane integrity [31, 32]. It is interesting to note that cholesterol depletion does not necessarily lead to an attenuated receptor internalization, as shown for the PTGER1 (PGE receptor) [32].

Besides its bronchospasmolytic and secretolytic properties there is one publication describing an anti-inflammatory effect on chronic bronchitis after EA 575® inhalation but the mode of action remains unclear and needs to be further investigated [33]

Since IL-6 is thought to play important roles in several inflammatory diseases which also refer to asthma and chronic bronchitis [34, 35], it was first checked for an inhibitory effect of EA 575® on IL-6 release from murine macrophages (J774.2).

As shown in the literature [36], J774.2 cells pre-treated with different concentrations of EA 575® and subsequently stimulated with LPS revealed a dose-dependent decrease in IL-6 release, statistically significant at 80 µg/ml. Pre-treatment with corticosterone served as control demonstrating an expected decrease in IL-6 release (Figure 9).

Expression and release of interleukins are mostly regulated through the NFκB pathway, so the influence of EA 575® on this pathway was measured first by immunostaining of NFκB subunit RelA. LPS induced translocation of NFκB in J774.2 cells was reduced by pre-treatment with 240 µg/ml EA575® (Figure 12). Similar results were obtained in HEK cells stimulated with TNFα (Figure 12). TNFα and LPS do not bind to the same receptor but their different signaling pathways both lead to NFκB translocation into the nucleus. Thus, EA 575® does not impact a single receptor pathway in inflammation, but rather manipulates processes to activate NFκB, like IKKβ mediated phosphorylation or NFκB:IκBα complex stability. NFκB transcriptional activity was measured as nanoluciferase activity in HEK cells stably transfected with a nanoluciferase coupled to an NFκB binding sequence. EA 575® dose-dependently inhibited TNFα-induced NFκB activity in these HEK Nanoluc-PEST cells at concentrations between 40 and 240 µg/ml (Figure 10). Similar to stimulation of TNFR1 in

HEK Nanoluc-PEST cells, stimulation of TLR4 with LPS in THP-1 Nanoluc-PEST cells led to an increased luciferase activity showing transcriptional activity of NFκB. This was dose-dependently inhibited by pre-incubation with EA 575® in concentrations between 80 and 240 µg/ml (Figure 11). TLR4 is a membrane associated receptor e.g. responsible for recognition of cell wall compounds of bacteria and signals through NFκB, even if the associated downstream kinases partially differ to that of TNFR1 pathway.

Schröfelbauer et al. demonstrated that glycyrrhizin, structural related to α-hedrin, also inhibits NFκB dependent cytokine secretion like TNFα and IFNγ from murine macrophages after TLR4 stimulation with LPS [37]. For the mode of action, they speculated that this finding results from an impact on membrane structures like lipid rafts, which are also important for TLR signaling [38]

For translocation and transcriptional activity of NFκB dissociation from its inhibitor IκBα is required. Therefore, IκBα is phosphorylated by IKKβ, which is arranged in a kinase complex with IKKα and their regulating unit NEMO (also called IKKγ). The phosphorylation site of IκBα is located at Ser32, which dictates its ubiquitination and subsequent degradation via the proteasome [17, 39].

In HEK cells stimulated for 10 min with TNFα, phosphorylation of IκBα at Ser32 was significantly lowered after pre-incubation with EA 575® (Figure 13), probably leading to an enhanced complex stability of NFκB:IκBα.

IKKβ also phosphorylates NFκB subunit RelA at Ser536. After pre-incubation with EA 575®, phosphorylation was continuously enhanced to a statistically significant level 10 min after TNFα stimulation (Figure 14).

While the phosphorylation of IκBα is commonly known to induce its dissociation from RelA, phosphorylation of RelA and the subsequent processes are more complex. Several phosphorylation sites are known and many of them positively regulate NFκB transcripitional activity [40] As one example for negative regulation, phosphorylation at Ser536 was shown to

reduce NFκB translocation into the nucleus and to reduce transcriptional activity [41]. While it is not completely clarified how the IKK complex is activated upon stimulation, it was shown that NEMO acts as a scaffold protein directing the kinase to its phosphorylation sites, e.g. to IκBα or RelA, thereby influencing the affinity of IKKβ to different target proteins [42]. This affinity can be changed, e.g., by target inaccessibility, which Schröfelbauer et al. demonstrated with a RelA mutant that could no longer be phosphorylated. They hypothesized that this also might be a regulation point which supports the inhibiting effect of a lower IκBα phosphorylation rate.

To investigate the effect of dropped phosphorylation of IκBα, the stability of NFκB:IκBα complex was measured in a protein fragment complementation (PFC) assay. Therefore, a HEK cell line was generated, overexpressing both RelA coupled to C-terminal part of Venus and IκBα coupled to N-terminal part of Venus as firstly described by Yu et al [8]. In unstimulated HEK cells IκBα remains in complex with RelA resulting in the formation of the fluorescence protein. Stimulation with TNFα induces dissociation of the complex and thereby also to decomposition of Venus, which can be measured as a fluorescence decrease (Figure 15). Compared to TNFα stimulation alone pre-incubation with EA 575® reduced the TNFα-induced decrease in fluorescence intensity, demonstrating a higher amount of assembled fluorescent Venus fragments and thus of the RelA:IκBα complex (Figure 16). Taken together, the findings presented in this work clearly indicate an impact of EA 575® on inflammatory processes through an inhibitory impact on the NFκB pathway.

As discussed above previous work dealing with EA 575® effects mostly focussed on the β_2AR pathway for its importance in bronchospasmolysis and secretolysis. This work focussed on the NFκB pathway for its crucial relevance in inflammation. These two pathways have been demonstrated in the literature to display crosstalk via the scaffold protein β-arrestin. It is thought to interact with IκBα, thereby probably stabilizing the complex with NFκB which results in an anti-inflammatory effect [22, 43, 44]. Since β-arrestin 2 recruitment was already shown to be influenced by EA 575® (see above) it seemed likely that EA 575® also affects

the crosstalk between the NFκB and β_2AR pathways. The influence of β_2AR stimulation on NFκB activity was primarily measured in the HEK Nanoluc-PEST cells. Cells were stimulated with terbutaline prior to TNFα stimulation, and NFκB transcriptional activity was measured through nanoluciferase activity. Terbutaline co-stimulation significantly inhibited NFκB transcriptional activity, which demonstrates the crosstalk between these pathways. Additional pre-incubation with EA 575® exhibited a synergistic inhibiting effect with terbutaline stimulation on TNFα induced NFκB transcriptional activity (Figure 17). To check whether this effect depends on β-arrestins the same experiments were performed in HEK β-arrestin 1/2 KO Nanoluc-PEST cells. Knock-out of β-arrestin 1/2 abolished the terbutaline induced drop in NFκB transcriptional activity after TNFα stimulation. This clearly shows that the inhibitory effect of terbutaline on NFκB transcriptional activity, and also the synergistic EA 575® effect, depends on β-arrestin. This finding is supported by glycyrrhizin, structural related to α-hederin, that was also shown to exhibit a synergistic effect with a β_2-agonist on NFκB transcriptional activity [45].

The synergistic effect of EA 575® and terbutaline, observed in HEK Nanoluc-PEST cells was absent as expected, in HEK β-arrestin 1/2 KO Nanoluc-PEST cells. In contrast the inhibiting effect of EA 575® pre-incubation on the NFκB transcriptional activity was found even in HEK β-arrestin 1/2 KO cells. Although it was not as pronounced as in HEK Nanoluc-PEST cells, it points on an additional, β-arrestin independent, influence of EA 575® on the NFκB pathway (Figure 18). This could also derive from extract ingredients that were shown previously to influence NFκB driven inflammatory processes. For example, rutin as well as 3,5- and 4,5-dicaffeoylquinic acid inhibit the NFκB dependent iNOS gene transcription and as a result the synthesis of nitric oxide whereas chlorogenic acid reduces LPS induced NFκB dependent cyclooxygenase-2 (COX-2) expression in RAW 264.7 cells [46-48]. Furthermore, 3,4-dicaffeoylquinic acid inhibits the phorbol-12-myristate-13-acetate induced COX-2 expression in RAW264.7 cells by blocking the catalytic activity of JNK/p38 MAP kinases and the activation of C/EBPβ and AP-1 [49]

As it was suggested by Witherow et al. and Gao et al. that the binding of β-arrestin to IκBα stabilizes the NFκB:IκBα complex [43, 44], this issue was investigated by PFC. The PFC assay confirmed that terbutaline stimulation enhanced complex stability of NFκB:IκBα under TNFα stimulating condition (Figure 19), but that β-arrestin knock-out did not change this effect (Figure 20). Thus, the assumed stabilizing effect of β-arrestin could not be confirmed [43, 44]. The data presented in this work show that the stabilizing effect of a β_2AR stimulation on the NFκB:IκBα complex is not β-arrestin dependent. Therefore, the inhibiting effect of β_2AR signaling on transcriptional NFκB activity seems to arrive from a downstream event of the NFκB pathway. Another possible explanation could be a dual impact of β_2AR signaling on the NFκB pathway. Thus, the stabilized complex would not depend on β-arrestins, while a further downstream event depends on β-arrestins and influences NFκB transcriptional activity. In consideration of the multiple binding partners of β-arrestin it seems likely that other proteins involved in the NFκB pathway are influenced by β-arrestin [50]. Therefore, the mechanisms by which β_2-agonists and EA575® impact the stability of NFκB:IκBα complex has to be further investigated.

In conclusion, the data presented in this work give information about the mode of action of EA575® induced inhibition of β_2AR internalization. Additionally the results clearly confirm an anti-inflammatory effect of EA 575® mediated through inhibition of the NFκB transcriptional activity. It is particularly notable that this effect could be heightened by co-stimulation with terbutaline, which is of relevance for chronic inflammatory diseases of the respiratory tract like asthma and COPD which are commonly treated with β_2-agonists.

6 References

1. Lang C, Rottger-Luer P, Staiger C. A valuable option for the treatment of respiratory diseases: review on the clinical evidence of the ivy leaves dry extract EA 575(R). Planta medica. 2015;81(12-13):968-74.

2. Schaefer A, Kehr MS, Giannetti BM, Bulitta M, Staiger C. A randomized, controlled, double-blind, multi-center trial to evaluate the efficacy and safety of a liquid containing ivy leaves dry extract (EA 575(R)) vs. placebo in the treatment of adults with acute cough. Die Pharmazie. 2016;71(9):504-9.

3. Sieben A, Prenner L, Sorkalla T, Wolf A, Jakobs D, Runkel F, et al. Alpha-hederin, but not hederacoside C and hederagenin from Hedera helix, affects the binding behavior, dynamics, and regulation of beta 2-adrenergic receptors. Biochemistry. 2009;48(15):3477-82.

4. Zeil S, Schwanebeck U, Vogelberg C. Tolerance and effect of an add-on treatment with a cough medicine containing ivy leaves dry extract on lung function in children with bronchial asthma. Phytomedicine. 2014;21(10):1216-20.

5. Suleyman H, Mshvildadze V, Gepdiremen A, Elias R. Acute and chronic antiinflammatory profile of the ivy plant, Hedera helix, in rats. Phytomedicine. 2003;10(5):370-4.

6. Yeh CH, Yang JJ, Yang ML, Li YC, Kuan YH. Rutin decreases lipopolysaccharide-induced acute lung injury via inhibition of oxidative stress and the MAPK-NF-kappa B pathway. Free radical biology and medicine. 2014;69:249-57.

7. Kyung TW, Lee JE, Shin HH, Choi HS. Rutin inhibits osteoclast formation by decreasing reactive oxygen species and TNF-alpha by inhibiting activation of NF-kappa B. Experimental and molecular medicine. 2008;40(1):52-8.

8. Yu H, West M, Keon BH, Bilter GK, Owens S, Lamerdin J, et al. Measuring drug action in the cellular context using protein-fragment complementation assays. Assay and drug development technologies. 2003;1(6):811-22.

9. Kallal L, Gagnon AW, Penn RB, Benovic JL. Visualization of agonist-induced sequestration and down-regulation of a green fluorescent protein-tagged beta2-adrenergic receptor. Journal of biological chemistry. 1998;273(1):322-8.

10. Alvarez-Curto E, Inoue A, Jenkins L, Raihan SZ, Prihandoko R, Tobin AB, et al. Targeted elimination of G proteins and arrestins defines their specific contributions to both intensity and duration of G protein-coupled receptor signaling. Journal of biological chemistry. 2016;291(53):27147-59.

11. Schulte-Michels J, Wolf A, Aatz S, Engelhard K, Sieben A, Martinez-Osuna M, et al. alpha-Hederin inhibits G protein-coupled receptor kinase 2-mediated phosphorylation of beta2-adrenergic receptors. Phytomedicine. 2016;23(1):52-7.

12. Iino M, Furugori T, Mori T, Moriyama S, Fukuzawa A, Shibano T. Rational design and evaluation of new lead compound structures for selective betaARK1 inhibitors. Journal of medicinal chemistry. 2002;45(11):2150-9.

13. Homan KT, Wu E, Wilson MW, Singh P, Larsen SD, Tesmer JJ. Structural and functional analysis of G protein-coupled receptor kinase inhibition by paroxetine and a rationally designed analog. Molecular pharmacology. 2014;85(2):237-48.

14. Schroder R, Janssen N, Schmidt J, Kebig A, Merten N, Hennen S, et al. Deconvolution of complex G protein-coupled receptor signaling in live cells using dynamic mass redistribution measurements. Nature biotechnology. 2010;28(9):943-50.

15. Krasel C, Bunemann MB, Lorenz K, Lohse MJ. beta-arrestin binding to the beta(2)-adrenergic receptor requires both receptor phosphorylation and receptor activation. Journal of biological chemistry. 2005;280(10):9528-35.

16. El-Guendy N, Sinai AP. Potential problems inherent in cell-based stable NF-kappaB-GFP reporter systems. Molecular and cellular biochemistry. 2008;312(1-2):147-55.

17. Brown K, Gerstberger S, Carlson L, Franzoso G, Siebenlist U. Control of I-kappa-B-alpha proteolysis by site-specific, signal-induced phosphorylation. Science. 1995;267(5203):1485-8.

18. Buss H, Dorrie A, Schmitz ML, Hoffmann E, Resch K, Kracht M. Constitutive and interleukin-1-inducible phosphorylation of p65 NF-kappa B at serine 536 is mediated by multiple protein kinases including I kappa B kinase (IKK)-alpha, IKK beta, IKK epsilon, TRAF family member-associated (TANK)-binding kinase 1 (TBK1), and an unknown kinase and couples p65 to TATA-binding protein-associated factor II31-mediated interleukin-8 transcription. Journal of biological chemistry. 2004;279(53):55633-43.

19. Wex E, Kollak I, Duechs MJ, Naline E, Wollin L, Devillier P. The long-acting beta (2)-adrenoceptor agonist olodaterol attenuates pulmonary inflammation. Brititish journal of pharmacology. 2015;172(14):3537-47.

20. Izeboud CA, Monshouwer M, van Miert ASJPAM, Witkamp RF. The beta-adrenoceptor agonist clenbuterol is a potent inhibitor of the LPS-induced production of TNF-alpha and IL-6 in vitro and in vivo. Inflammation research. 1999;48(9):497-502.

21. Theron AJ, Steel HC, Tintinger GR, Feldman C, Anderson R. Can the anti-inflammatory activities of beta 2-agonists be harnessed in the clinical setting? Drug design, development and therapy. 2013;7:1387-98.

22. Kizaki T, Izawa T, Sakurai T, Haga S, Taniguchi N, Tajiri H, et al. beta(2)-Adrenergic receptor regulates Toll-like receptor-4-induced nuclear factor-kappa B activation through beta-arrestin 2. Immunology. 2008;124(3):348-56.

23. Baeuerle PA, Baltimore D. I-kappa-B - a specific inhibitor of the NF-kappa-B transcription factor. Science. 1988;242(4878):540-6.

24. Krasel C, Vilardaga JP, Bunemann M, Lohse MJ. Kinetics of G-protein-coupled receptor signalling and desensitization. Biochemical society transactions. 2004;32(Pt 6):1029-31.

25. Guo S, Carter RL, Grisanti LA, Koch WJ, Tilley DG. Impact of paroxetine on proximal beta-adrenergic receptor signaling. Cellular signalling. 2017;38:127-33.

26. Schroder R, Schmidt J, Muller A, Hennen S, Mohr K, Kostenis E. Label-free dynamic mass redistribution (DMR) technology is competent to reflect GPCR signaling through all main G protein coupling classes (G alpha(s), G alpha(l/o), G alpha(q/11) G alpha(12/13)). Naunyn-Schmiedebergers archive of pharmacology. 2011;383:38.

27. Shi Q, Hou YY, Yang Y, Bai G. Protective Protective effects of glycyrrhizin against beta(2)-adrenergic receptor agonist-induced receptor internalization and cell apoptosis. Biological and pharmaceutical bulletin. 2011;34(5):609-17.

28. Lorent J, Lins L, Domenech O, Quetin-Leclercq J, Brasseur R, Mingeot-Leclercq MP. Domain formation and permeabilization induced by the saponin alpha-hederin and its aglycone hederagenin in a cholesterol-containing bilayer. Langmuir. 2014;30(16):4556-69.

29. Rodal SK, Skretting G, Garred O, Vilhardt F, van Deurs B, Sandvig K. Extraction of cholesterol with methyl-beta-cyclodextrin perturbs formation of clathrin-coated endocytic vesicles. Molecular biology of the cell. 1999;10(4):961-74.

30. Subtil A, Gaidarov I, Kobylarz K, Lampson MA, Keen JH, McGraw TE. Acute cholesterol depletion inhibits clathrin-coated pit budding. Proceedings of the national academy of science of the USA. 1999;96(12):6775-80.

31. Pontier SM, Percherancier Y, Galandrin S, Breit A, Gales C, Bouvier M. Cholesterol-dependent separation of the beta(2)-adrenergic receptor from its partners determines signaling efficacy. Journal of biological chemistry. 2008;283(36):24659-72.

32. DiPilato LM, Zhang J. The role of membrane microdomains in shaping beta(2)-adrenergic receptor-mediated cAMP dynamics. Molecular biosystems. 2009;5(8):832-7.

33. Rudkowski ZL, T. Inhalationsbehandlung chronischer Bronchitiden im Kindesalter mit Prospan. Ärztliche Praxis. 1979;31(10):5.

34. Bucchioni E, Kharitonov SA, Allegra L, Barnes PJ. High levels of interleukin-6 in the exhaled breath condensate of patients with COPD. American journal of respiratory and critical care medicine. 2003;97(12):1299-302.

35. Rincon M, Irvin CG. Role of IL-6 in asthma and other inflammatory pulmonary Diseases. International journal of biological sciences. 2012;8(9):1281-90.

36. Schulte-Michels J, Runkel F, Gokorsch S, Haberlein H. Ivy leaves dry extract EA 575(R) decreases LPS-induced IL-6 release from murine macrophages. Die Pharmazie. 2016;71(3):158-61.

37. Schrofelbauer B, Raffetseder J, Hauner M, Wolkerstorfer A, Ernst W, Szolar OHJ. Glycyrrhizin, the main active compound in liquorice, attenuates pro-inflammatory responses by interfering with membrane-dependent receptor signalling. Biochemical journal. 2009;421(3):473-82.

38. Schmitz G, Orso E. CD14 signalling in lipid rafts: new ligands and co-receptors. Current opinion in lipidology. 2002;13(5):513-21.

39. Traenckner EBM, Pahl HL, Henkel T, Schmidt KN, Wilk S, Baeuerle PA. Phosphorylation of human I-kappa-B-alpha on serine-32 and serine-36 controls I-kappa-B-alpha proteolysis and NF-kappa-B activation in response to diverse stimuli. European molecular biology organization journal. 1995;14(12):2876-83.

40. Christian F, Smith EL, Carmody RJ. The regulation of NF-kappa B subunits by phosphorylation. Cells. 2016;5(1).

41. Moreno R, Sobotzik JM, Schultz C, Schmitz ML. Specification of the NF-kappa B transcriptional response by p65 phosphorylation and TNF-induced nuclear translocation of IKK epsilon. Nucleic acids research. 2010;38(18):6029-44.

42. Schrofelbauer B, Polley S, Behar M, Ghosh G, Hoffmann A. NEMO ensures signaling specificity of the pleiotropic IKKbeta by directing its kinase activity toward IkappaBalpha. Molecular cell. 2012;47(1):111-21.

43. Witherow DS, Garrison TR, Miller WE, Lefkowitz RJ. beta-Arrestin inhibits NF-kappa B activity by means of its interaction with the NF-kappa B inhibitor I kappa B alpha. Proceedings of the national academy of science of the USA. 2004;101(23):8603-7.

44. Gao H, Sun Y, Wu YL, Luan B, Wang YY, Qu B, et al. Identification of beta-arrestin2 as a G protein-coupled receptor-stimulated regulator of NF-kappa B pathways. Molecular cell. 2004;14(3):303-17.

45. Yang Y, Shi Q, Liu Z, Li RJ, Pan PW, Hou YY, et al. The synergistic anti-asthmatic effects of glycyrrhizin and salbutamol. Acta pharmacologica sinica. 2010;31(4):443-9.

46. Kazlowska K, Hsu T, Hou CC, Yang WC, Tsai GJ. Anti-inflammatory properties of phenolic compounds and crude extract from Porphyra dentata. Journal of ethnopharmacology. 2010;128(1):123-30.

47. Shan J, Fu J, Zhao Z, Kong X, Huang H, Luo L, et al. Chlorogenic acid inhibits lipopolysaccharide-induced cyclooxygenase-2 expression in RAW264.7 cells through suppressing NF-kappaB and JNK/AP-1 activation. International immunopharmacology. 2009;9(9):1042-8.

48. Park KH, Park M, Choi SE, Jeong MS, Kwon JH, Oh MH, et al. The anti-oxidative and anti-inflammatory effects of caffeoyl derivatives from the roots of Aconitum koreanum R.. Biological and pharmaceutical bulletin. 2009;32(12):2029-33.

49. Han EH, Kim JY, Kim HG, Chun HK, Chung YC, Jeong HG. Inhibitory effect of 3-caffeoyl-4-dicaffeoylquinic acid from Salicornia herbacea against phorbol ester-induced cyclooxygenase-2 expression in macrophages. Chemico-biological interactions. 2010;183(3):397-404.

50. Xiao K, McClatchy DB, Shukla AK, Zhao Y, Chen M, Shenoy SK, et al. Functional specialization of beta-arrestin interactions revealed by proteornic analysis. Proceedings of the national academy of science of the USA. 2007;104(29):12011-6.

7 Appendix

7.1 Supplemental material

Table S 1: Retention times of identified substances in EA 575® CID-100048

Substance	Retention time in EA 575® chromatogram [min]	Retention time of reference substance [min]
Rutin	24.85	24.04
3,4 DCA	27.38	26.16
Kaempferol-3-O-rutinoside	27.93	28.04
3,5 DCA	28.45	27.28
4,5 DCA	29.94	29.10
Hederacoside C	34.31	34.04
Hederacoside D	34.68	34.45
Hederacoside B	36.83	36.56
α-Hederin	43.08	41.79

Table S 2: HPLC determination of α-hederin reference substance

	Reference measurement 1	Reference measurement 2
Sum of area of integrated peaks	8722.38	8664.47
Area under peak of α-hederin	7157.09	7160.92
Calculated purity [%]	82.05	82.65
Injected amount [µg]	25.8	25.8
Area equal to 1 µg	338.04	335.82

Table S 3: Calculation of α-hederin amount in EA 575® CID-100048

	Extract analysis 1	Extract analysis 2
α-Hederin peak area	105.92	107.34
Calculated amount [%]	0.785	0.796

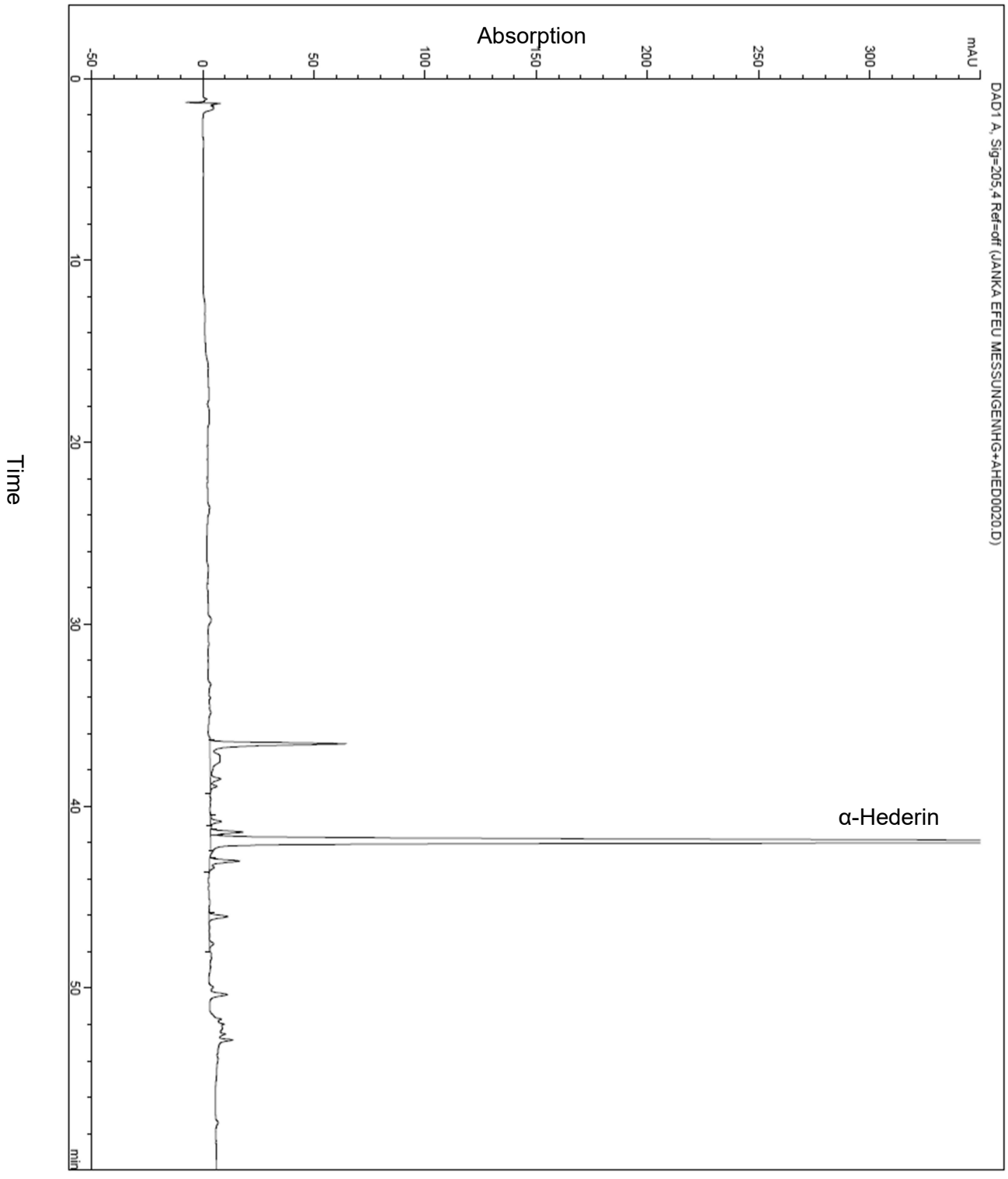

Figure S 1: Representative HPLC chromatogram of α-hederin reference substance. Chromatogram was obtained by the method described in chapter 3.1

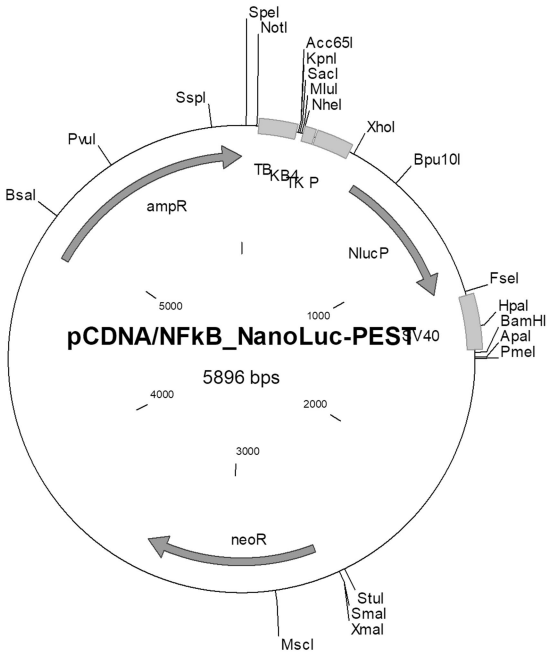

Figure S 2: Nanoluc-PEST plasmid card, pNF-KB-D2EGFP vector was used as template (Clontech, Mounten View, California, USA), Nanoluc-PEST sequence was cut from pNL1.2[NlucP] (Promega, Madison, Wisconsin, USA).

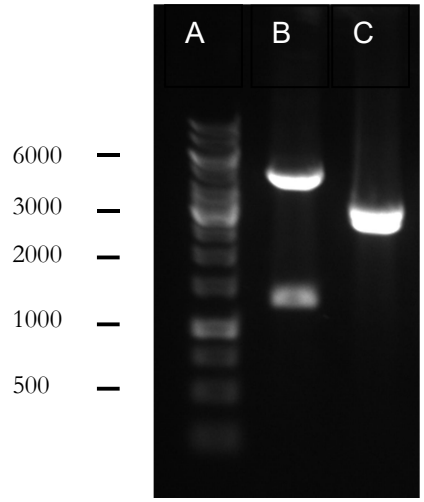

Figure S 3: Agarose gel analysis of enzymatic digestions A) 1 kb DNA ladder (Thermo Fisher Scientific), B) Nanoluc-PEST digested by BglI expected band sizes 4597+1299 bp C) Nanoluc-PEST digested by PstI expected band sizes 3155+2741 bp. Both restriction enzymes were obtained from Thermo Fisher Scientific

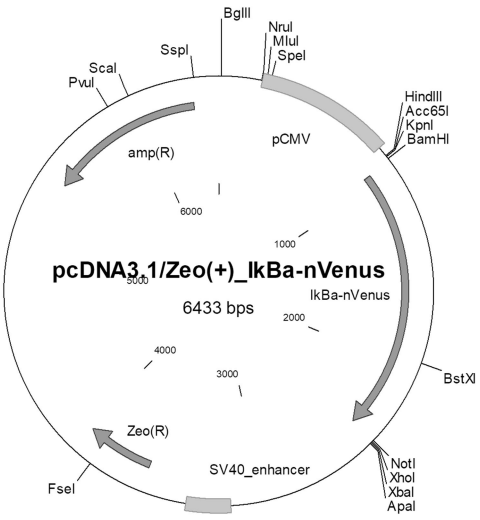

Figure S 4: pCDNA3.1/Zeo_IkBa-nVenus plasmid card, plasmid was constructed by GeneArt (Regensburg, Germany).

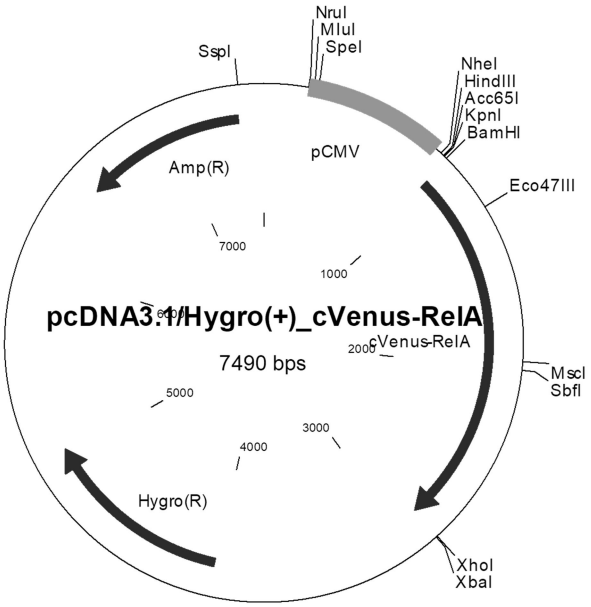

Figure S 5: pCDNA3.1/Hygro_cVenus-RelA plasmid card, plasmid was constructed by GeneArt (Regensburg, Germany).

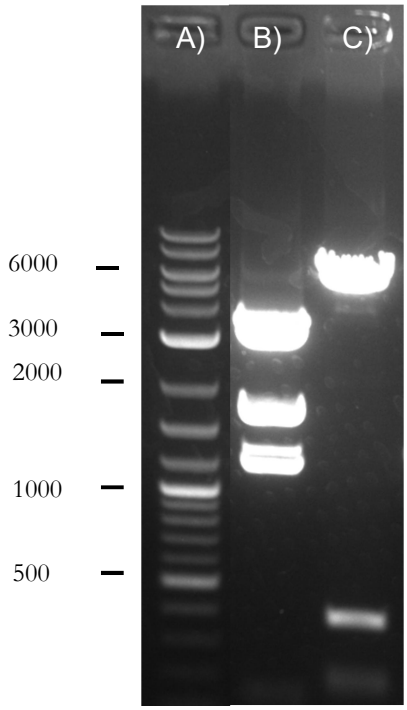

Figure S 6: Agarose gel analysis of enzymatic digestions A) Quick-Load® Purple 2-Log DNA Ladder (0.1 - 10.0 kb) (NEB, Ipswich, Massachusetts, USA), B) pCDNA3.1/Zeo_IkBa-nVenus digested by BglI expected band sizes 3374, 1723, 1143, 122, 71 bp C) pCDNA3.1/Zeo_IkBa-nVenus digested by PstI; expected band sizes 5395, 354, 351, 183, 150 bp. Both restriction enzymes were obtained from Thermo Fisher Scientific.

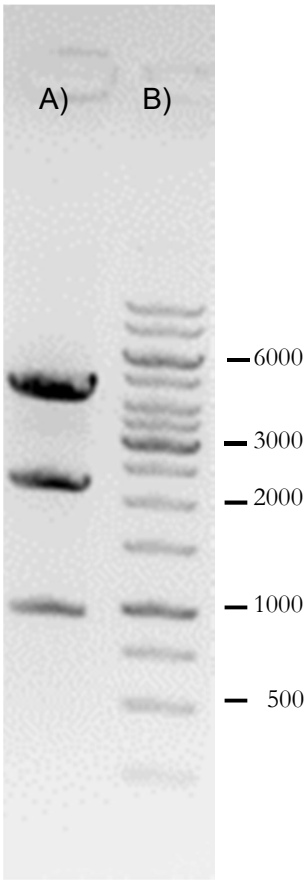

Figure S 7: Agarose gel analysis of enzymatic digestion A) pCDNA3.1/Hygro_c-Venus-RelA digested by EcoRI, expected band sizes 4375, 2182, 933 bp, B) 1 kb DNA ladder (Thermo Fisher Scientific) Restriction enzyme was obtained from Thermo Fisher Scientific.

CompactPrep® Plasmid Kits

CompactPrep Plasmid Kits (cat. nos. 12843 and 12863) can be stored at room temperature (15–25°C) for up to 2 years.

For more information, please refer to the *CompactPrep Plasmid Purification Handbook*, which can be found at www.qiagen.com/handbooks.

For technical assistance, please call toll-free 00800-22-44-6000, or find regional phone numbers at www.qiagen.com/contact.

Notes before starting

- Add RNase A solution to Buffer P1 to a final concentration of 100 µg/ml.
- **Optional**: Add LyseBlue® reagent to Buffer P1 at a ratio of 1:1000.
- Add ethanol (96–100%) to Buffer PE before use (see bottle label for volume).
- Dissolve precipitates in Buffer P2 and Buffer BB by warming to 37°C.
- Close the bottle containing Buffer P2 immediately after use.
- All microcentrifugation steps are carried out at 10,000 x *g* (approximately 13,000 rpm) in a conventional tabletop microcentrifuge.
- Symbols: ■ 200 µg high-copy plasmid DNA using the CompactPrep Plasmid Midi Kit; ▲ 750 µg plasmid DNA using the CompactPrep Plasmid Maxi Kit.

Table 1. Maximum recommended Luria Bertani (LB) culture volumes

Plasmid	CompactPrep Plasmid Midi	CompactPrep Plasmid Maxi
High-copy	25 ml	100 ml
Low-copy	50 ml	250 ml

1. Harvest the bacterial cells by centrifugation at 6000 x *g* for 15 min at 4°C.
2. Completely resuspend the bacterial pellet in ■ 2 ml or ▲ 5 ml Buffer P1.
3. Add ■ 2 ml or ▲ 5 ml Buffer P2, mix thoroughly by vigorously inverting the sealed tube 4–6 times, and incubate at room temperature (15–25°C) for 3 min. If LyseBlue reagent has been added, the cell suspension will turn blue.
4. Add ■ 2 ml or ▲ 5 ml Buffer S3 to the lysate, and mix immediately by vigorously inverting 4–6 times. Proceed directly to step 5. Do not incubate the lysate on ice. If LyseBlue reagent has been added, mix the solution until it is completely colorless.
5. Centrifuge at ≥20,000 x *g* for 30 min at 4°C. Remove supernatant containing plasmid DNA promptly.
6. Centrifuge the supernatant again at ≥20,000 x *g* for 15 min at 4°C. Remove supernatant containing plasmid DNA promptly.
7. During incubation, prepare the vacuum manifold and CompactPrep Midi or Maxi columns.
8. Add ■ 2 ml or ▲ 5 ml Buffer BB to the lysate. Mix by inverting 4–6 times and transfer the adjusted lysate into a tube extender attached to the CompactPrep column.
9. Switch on vacuum source to draw the solution through the CompactPrep column and then switch off vacuum source.
10. Wash the DNA using a microcentrifuge (step 10a) or using a vacuum manifold (step 10b).

10 a. To wash the DNA using a microcentrifuge: Discard the tube extenders and place the CompactPrep column into a 2 ml collection tube. Wash by adding 0.7 ml Buffer PE and centrifuging for 30–60 s. Discard the flow-through, and centrifuge for an additional 1 min.

10 b. To wash the DNA using a vacuum manifold: Discard the tube extenders. Add 0.7 ml Buffer PE and switch on the vacuum manifold. To completely remove residual buffer, apply vacuum for an additional 10 min.

11. Place the CompactPrep column in a clean 1.5 ml microcentrifuge tube. To elute DNA, add ■ 100 µl or ▲ 200 µl of Buffer EB (10 mM Tris·Cl, pH 8.5) or water to the center of the CompactPrep column, let stand for 1 min, then centrifuge for 1 min.

Figure S 8: Quick start protocol for CompactPrep Midi Prep (Qiagen®). For more detailed protocol visit https://www.qiagen.com/us/shop/sample-technologies/dna/plasmid-dna/compactprep-plasmid-midi-kits/#orderinginformation

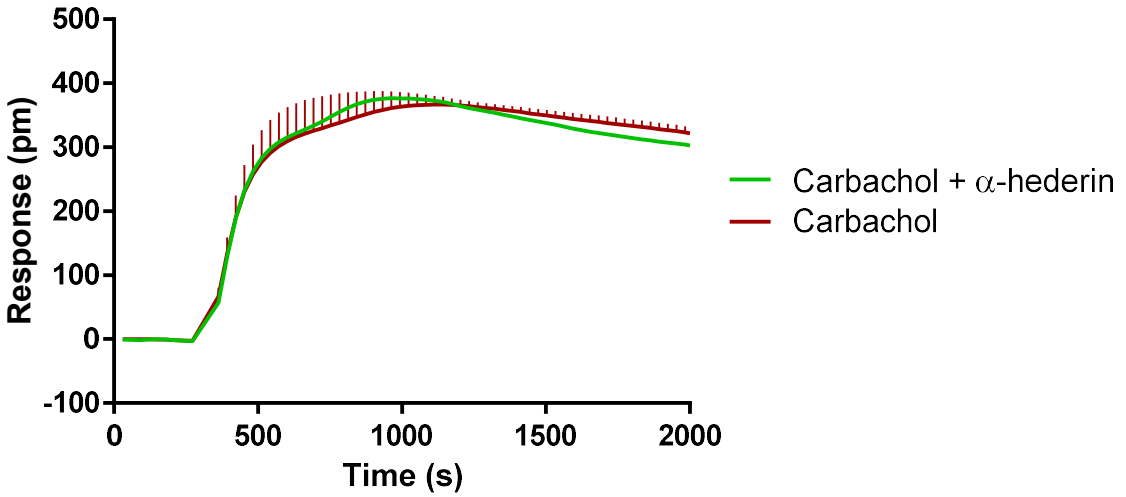

Figure S 9: Influence of overnight pre-incubation with 1 µM α-hederin on carbachol induced dynamic mass redistribution measurement in HEK β_2AR GFP cells. Carbachol stimulation was performed with 100 µM after baseline acquisition for 300 s.

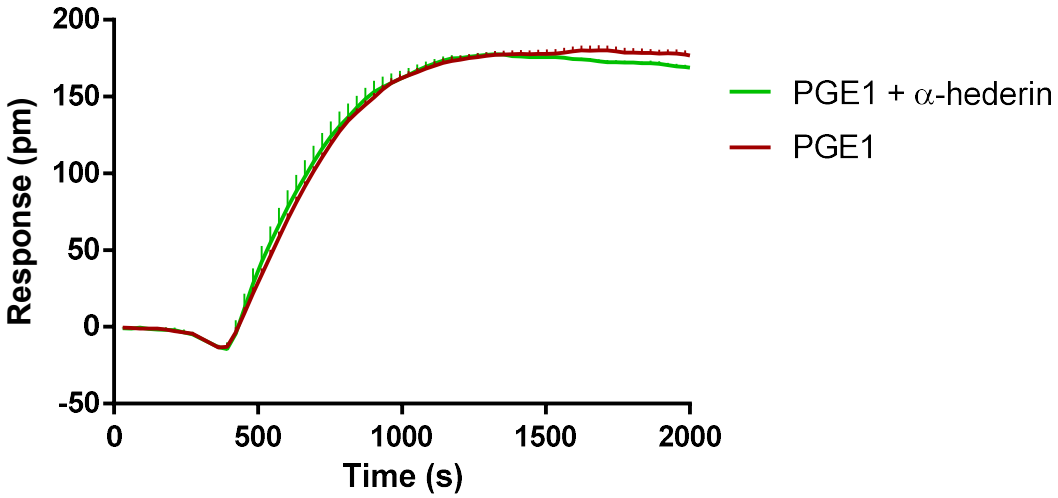

Figure S 10: Influence of overnight pre-incubation with 1 µM α-hederin on PGE1 induced dynamic mass redistribution measurement in HEK β_2AR GFP cells. PGE1 stimulation was performed with 10 µM after baseline acquisition for 300 sec.

QUICK-START PROCEDURE: ALLOSTERIC MODULATOR DOSE RESPONSE

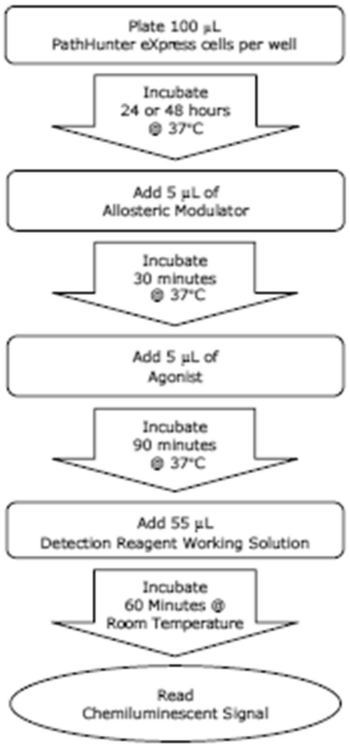

*Please refer to the cell line specific datasheet for any variation in assay conditions.

SUBSTRATE PREPARATION AND ADDITION

1. During the incubation period, prepare a working stock of PathHunter Detection Reagents by mixing **19 parts** Cell Assay Buffer, **5 parts** Substrate Reagent 1 and **1 part** Substrate Reagent 2.

Component	Entire Plate (96 wells)
Cell Assay Buffer	4.75 mL
Substrate Reagent 1	1.25 mL
Substrate Reagent 2	0.25 mL

NOTE:
The working solution is stable for up to 8 hours at room temperature.

2. Add 55 µL of prepared detection reagent per well and incubate for 60 minutes at room temperature (23°C). **DO NOT pipette up and down in the well to mix or vortex/shake plates.**
3. Read samples on any standard luminescence plate reader.
4. Use GraphPad Prism® or other comparable program to plot your agonist dose response.

Figure S 11: Assay relevant abstracts of PathHunter® eXpress β-Arrestin Human and Ortholog GPCR Assays. For whole manual visit: https://www.discoverx.com/tools-resources/document-resource-library/documents/updated-cell-culture-protocol-technical-bulletin

Determine the number of 8-well strips required for the assay. Insert the strips in the frames for use. Re-bag any unused strips and frames, and store at 2 to 8°C for future use.

Bind antigen

1. Add 100 µL of standards, TC samples or controls to the appropriate microtiter wells. For sera and plasma samples, add 50 µL of standard diluents to the appropriate microtiter wells followed by 50 µL of sample.
2. Cover the plate with plate cover and incubate for 2 hours at room temperature.
3. Thoroughly aspirate the solution and wash wells 4 times with diluted Wash Buffer.

Add detector antibody

4. Add 100 µL Ms IL-6 Biotin Conjugate solution into each well except chromogen blanks.
5. Cover the plate with plate cover and incubate for 30 minutes at room temperature.
6. Thoroughly aspirate the solution and wash wells 4 times with diluted Wash Buffer.

Add Streptavidin-HRP

7. Add 100 µL Streptavidin-HRP (see page 2) into each well except the chromogen blanks.
8. Cover the plate with plate cover and incubate for 30 minutes at room temperature.
9. Thoroughly aspirate the solution and wash wells 4 times with diluted Wash Buffer.

Add chromogen

10. Add 100 µL Stabilized Chromogen to each well. The substrate solution will begin to turn blue.
11. Cover the plate with plate cover and incubate for 30 minutes at room temperature **in the dark**.

Note: TMB should not touch aluminum foil or other metals.

Add stop solution

12. Add 100 µL Stop Solution to each well. Tap side of the plate gently to mix. The solution in the wells changes from blue to yellow.

Read the plate and generate the standard curve

1. Read the absorbance at 450 nm. Read the plate within 2 hours after adding the Stop Solution.
2. Use curve-fitting software to generate the standard curve. A four parameter algorithm provides the best standard curve fit. Optimally, the background absorbance may be subtracted from all data points, including standards, unknowns and controls, prior to plotting.
3. Read the concentrations for unknown samples and controls from the standard curve. Multiply value(s) obtained for sample(s) by the appropriate factor to correct for the sample dilution.

   Note: Dilute samples producing signals greater than that of the highest standard in Standard Diluent Buffer and reanalyze. Multiply the concentration by the appropriate dilution factor.

Figure S 12: Assay relevant abstracts of Novex Mouse IL-6 ELISA kit. For whole manual visit: http://www.thermofisher.com/order/catalog/product/KMC0061

Promega

4. Nano-Glo® Luciferase Assay System Protocols

4.A. Preparation of the Nano-Glo® Luciferase Assay Reagent

Remove the Nano-Glo® Luciferase Assay Substrate from storage and mix by pipetting. Thaw the Nano-Glo® Luciferase Assay Buffer if stored at –20°C but do **not** exceed 25°C. Prepare the desired amount of reconstituted Nano-Glo® Luciferase Assay Reagent by combining one volume of Nano-Glo® Luciferase Assay Substrate with 50 volumes of Nano-Glo® Luciferase Assay Buffer. For example, if the experiment requires 10ml of reagent, add 200µl of substrate to 10ml of buffer.

Notes:

1. If the Nano-Glo® Luciferase Assay Substrate has collected in the cap or on the sides of the tube, briefly spin tubes containing 200µl or 1ml of substrate in a microcentrifuge. Place 4ml tubes in a swinging bucket rotor and centrifuge at 200 × *g* for 1 minute.
2. We recommend preparing the Nano-Glo® Luciferase Assay Reagent fresh for each use rather than storing the reagent at any temperature.
3. Once reconstituted, the reagent will lose 10% activity in approximately 8 hours and 50% activity in approximately 2 days at room temperature. The reconstituted reagent may be stored at 4°C with <10% decrease in activity over 2 days.

4.B. Detection of NanoLuc® Luciferase in Mammalian Cells (Lytic Method)

1. Allow all assay components (reagent and sample) to equilibrate to room temperature prior to assay. For example, remove a tissue culture plate from the 37°C, 5% CO_2 incubator and equilibrate it to room temperature for 5–10 minutes.
2. Add one volume of Nano-Glo® Luciferase Assay Reagent equal to the volume of the sample and mix for optimal consistency.
3. Wait at least 3 minutes before measuring luminescence. The luminescence intensity will decay gradually, with a signal half-life of approximately 120 minutes at room temperature.

Notes:

1. At high expression levels, the luminescence signal half-life can decrease significantly due to rapid depletion of the furimazine substrate (see Section 5.A). Experimental conditions should be modified to avoid extremely high expression (see Section 5.B).
2. Ensure that the instrument is operating within its linear dynamic range when measuring luminescence (see Section 5.C). Consult with the instrument manufacturer or determine this range empirically. Many instruments will not indicate if values are outside of the linear range.
3. The Nano-Glo® Luciferase Assay System is compatible with a variety of components used in mammalian cell culture experiments, showing minimal differences in luminescence intensity or signal half-life (Figure 5).

Figure S 13: Assay relevant abstracts of NanoGlo Luciferase assay system. For whole manual visit: https://www.promega.com/-/media/files/resources/protocols/technical-manuals/101/nanoglo-luciferase-assay-system-protocol.pdf

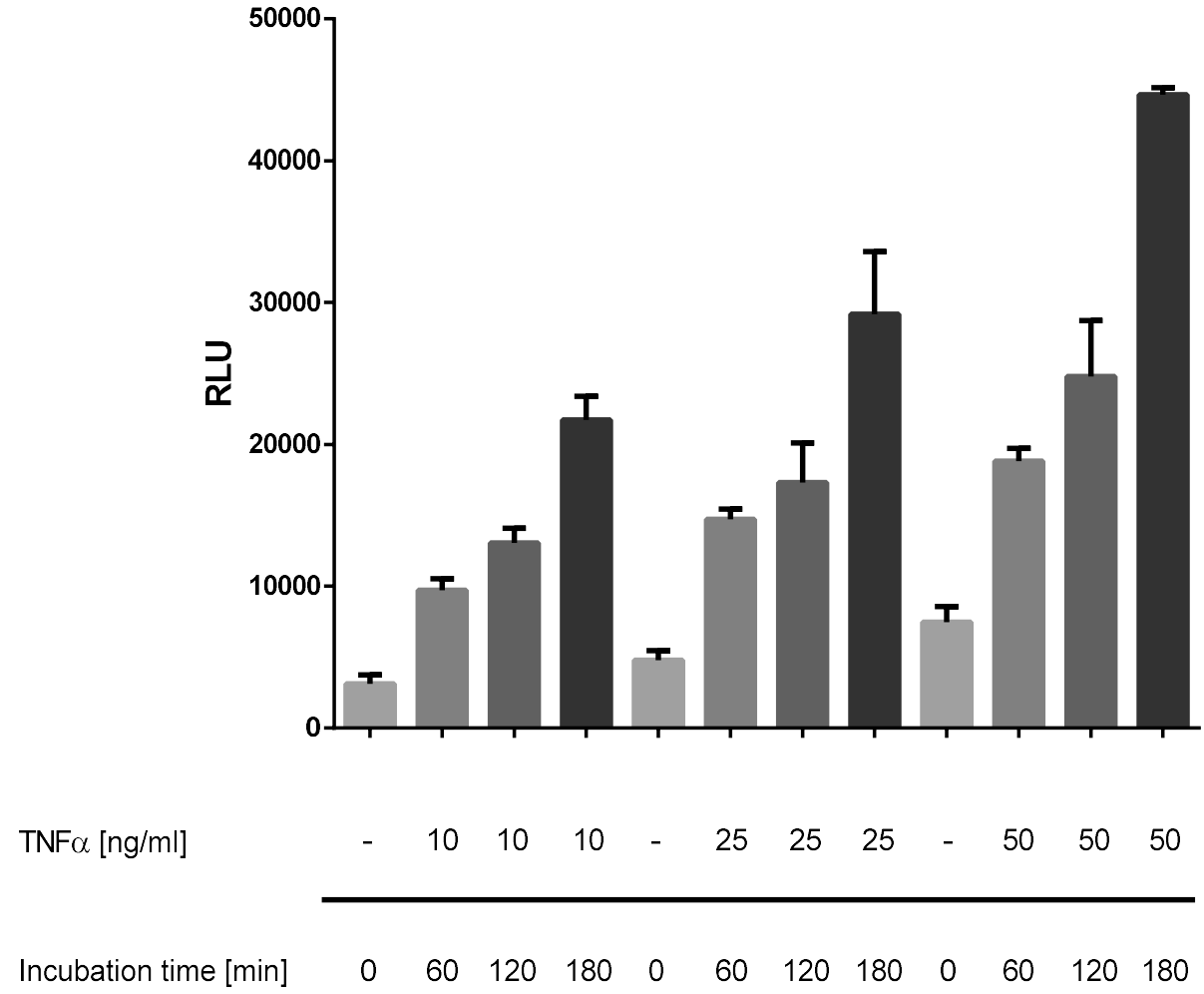

Figure S 14: Time- and dose-dependent NFκB transcriptional activity in TNFα stimulated HEK Nano-PEST cells.

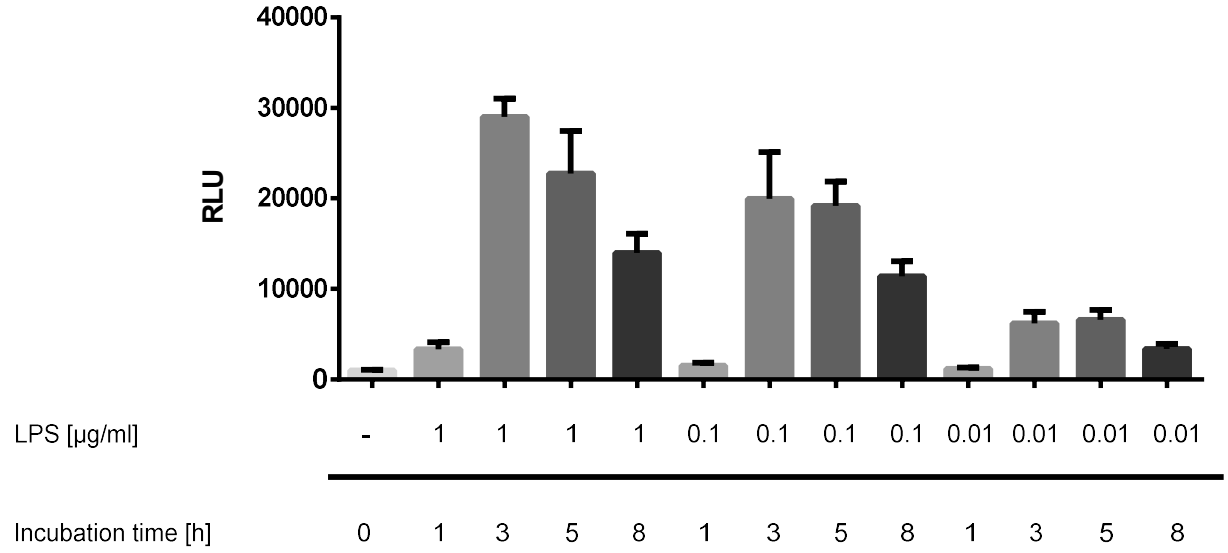

Figure S 15: Time- and dose-dependent NFκB transcriptional activity in LPS stimulated THP-1 Nano-PEST cells.

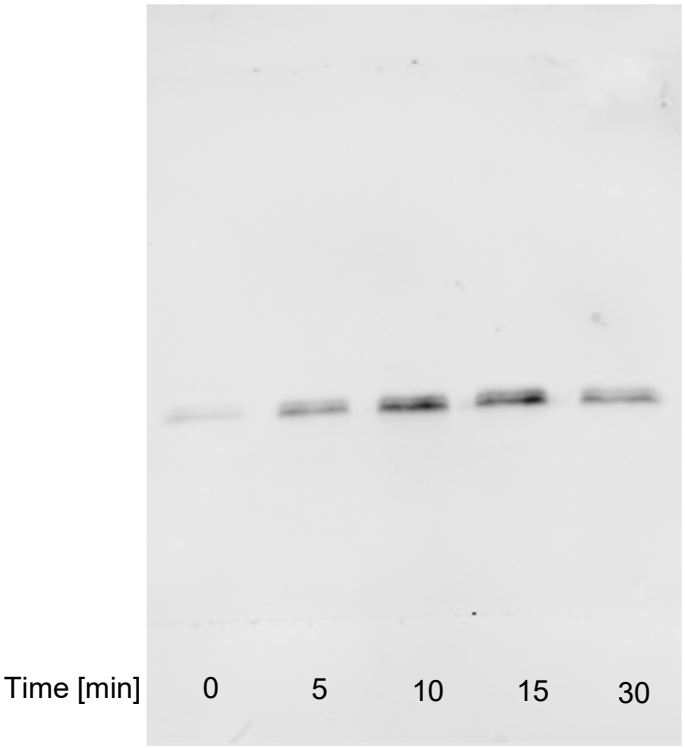

Figure S 16: Western blot of Ser536 phosphorylated RelA stimulated for the indicated time with 25 ng/ml TNFα.

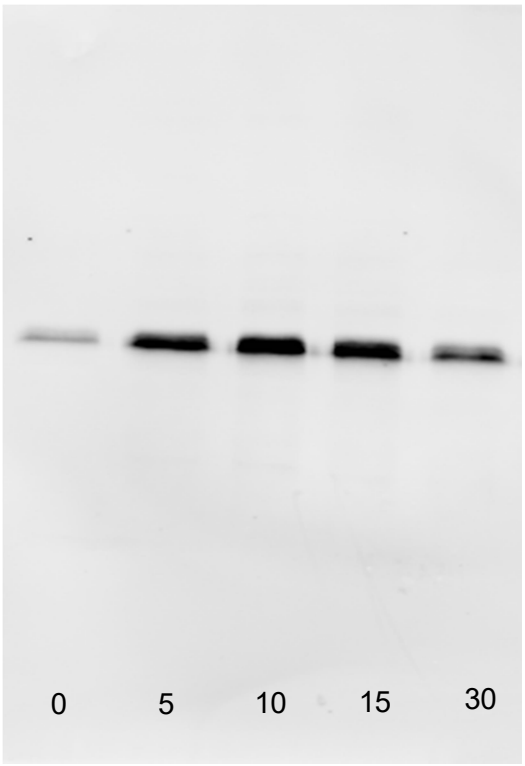

Figure S 17: Western blot of Ser536 phosphorylated RelA stimulated for the indicated time with 25 ng/ml TNFα and pre-incubated for 8 h with 240 µg/ml EA 575®

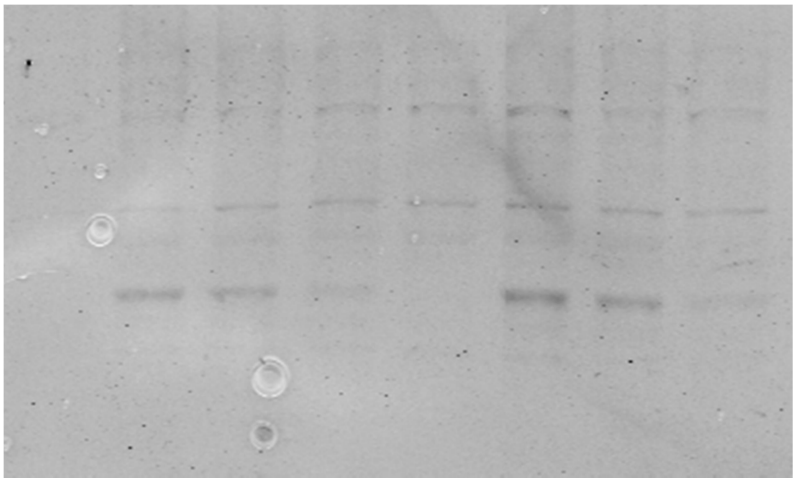

Time [min]	0	5	10	15	0	5	10	15
EA 575®	+	+	+	+	-	-	-	-

Figure S 18: Western blot of Ser32 phosphorylated IκBα stimulated for the indicated time with 25 ng/ml TNFα and with or without pre-incuabtion with 240 µg/ml EA 575® for 8 h.

Protocol for Single Color Target Detection

Use this protocol to detect targets in the 800 nm channel only.

1. Prepare Kit reagents by adding the appropriate volume of methanol as indicated on each bottle.

   Add 30 mL of methanol to the Total Protein Stain bottle
   Add 60 mL of methanol to each of the Wash and Reversal Solution bottles

2. After transfer, rinse the membrane in laboratory grade water. For a dried membrane:
   Nitrocellulose: wet with laboratory grade water.
   PVDF: wet with methanol, then water.

3. Incubate the membrane in 5 mL of Total Protein Stain for 5 minutes, with gentle shaking.

4. Decant Total Protein Stain thoroughly. Rinse the membrane twice in Wash Solution.

5. Image membrane in the 700 nm channel on an Odyssey Imaging System (or equivalent).

6. Process the membrane as usual for blocking and immunodetection, using IRDye® secondary antibodies for target detection in the 800 nm channel.

   NOTE: Visible color from stain will wash off during processing.

7. Image membrane in the appropriate channel(s) on an Odyssey Imaging System (or equivalent).

8. Proceed to "Analysis with Image Studio™ Software".

Analysis with Image Studio™ Software

1. On the Total Protein Stain image in the 700 nm channel, use the *Draw Rectangle* tool under Analysis → Shape. Draw a rectangle around the entire first lane on the blot image.

   - Copy and paste this shape or use the Add Selection Tool to each of the remaining sample lanes.
     NOTE: If lanes are skewed on the blot image, shapes can be rotated to line up better with each lane using the Edit → Rotate tool.
   - Quantify the background-subtracted Signal of each lane as directed in the Image Studio Help System and support documentation.

2. On the Western blot image, quantify the background-subtracted Signal of the target bands in the 700 and/or 800 nm channel(s) as directed in the Image Studio Help System and support documentation.

3. Export the appropriate quantitation data from both sets of images (the Total Protein Stain image and the Western blot image(s)) to Microsoft® Excel or similar program.

4. Calculate Normalization Factors for the Total Protein Stain blot image data: (Normalization Factors ≤ 1). Each lane will have its own Normalization Factor:

$$\frac{Signal\ for\ each\ lane}{Signal\ for\ lane\ with\ highest\ Signal} = Lane\ Normalization\ Factor$$

5. Calculate the Normalized Signal for each band in the Western blot image, using the corresponding Lane Normalization Factor:

$$\frac{Target\ Band\ Signal}{Lane\ Normalization\ Factor} = Normalized\ Signal$$

Figure S 19: Assay relevant abstracts of REVERT Total protein stain kit. For whole manual visit: https://www.licor.com/bio/pack_inserts/get_pack?filename=926-11010_REVERTTotalProteinStainKit_988-15930_1459353647.pdf

7.2 Publications

- Schulte-Michels J, Wolf A, Aatz S, Engelhard K, Sieben A, Martinez-Osuna M, et al. alpha-Hederin inhibits G protein-coupled receptor kinase 2-mediated phosphorylation of beta2-adrenergic receptors. Phytomedicine. 2016;23(1):52-7.
- Schulte-Michels J, Runkel F, Gokorsch S, Haberlein H. Ivy leaves dry extract EA 575(R) decreases LPS-induced IL-6 release from murine macrophages. Die Pharmazie. 2016;71(3):158-61.
- Schulte-Michels J, Keksel C, Haberlein H, Franken S. Anti-inflammatory effects of ivy leaves dry extract: influence on transcriptional activity of NFkappaB. Inflammopharmacology. 2018. Epub 2018/05/12.

7.3 Poster

- α- Hederin, an indirect GRK2 inhibitor, inhibits desensityzation of β_2 adrenergic receptor under stimulating conditions, Janka Schulte-Michels, Felix Häberlein, Hanns Häberlein, Glisten Meeting 06.-08. April 2016, Erlangen
- Cellular evidence for EA 575 as an add-on therapy for chronic inflammations of the lower respiratory tract, Janka Schulte-Michels, Hanns Häberlein, Sebastian Franken, 59. Kongress der DPG, 14.-17. March 2018, Dresden

7.4 Danksagung

Vielen Dank, Hanns, für die engagierte Betreuung der Doktorarbeit und die Bereitstellung des Themas. Die vielen Freiheiten und der Respekt den du deinen Doktorand*innen entgegenbringst haben die vier Jahre in deiner Arbeitsgruppe zu einer tollen Zeit gemacht, auch wenn es mal nicht so lief.

Vielen Dank auch Frau Prof. Dr. Evi Kostenis für die Übernahme des Koreferats. Des Weiteren danke ich Ihnen für die Bereitstellung des DMR-, sowie des Ensight readers und der β-arrestin knock-out Zellen, die einen großen Gewinn für meine Forschungsarbeit ausmachten.

Meinen Kolleg*innen im Institut für Biochemie und Molekularbiologie sowie ganz besonders Nelli, Thomas, Hendrik, Stefan und Sebastian danke ich für immer gute Laune und konstruktive Problemlösung. Vor allem Sebastian möchte ich in diesem Zuge auch für die praktische Unterstützung bei sämtlichen Laborarbeiten danken.

Den Mitarbeiter*innen der Arbeitsgruppe Kubitscheck, vor allem Jan-Peter Siebrasse und Jan Ruland, danke ich für die Bereitstellung der Mikroskope sowie der ständigen Hilfestellung bei Problemen. Auch wenn das FRET Experiment am Ende leider nicht funktioniert hat, ward ihr mir eine große Hilfe.

Zuletzt noch ein großer Dank an meinen Vater, meine Schwester und meinen Mann, die mir immer, bewusst und unbewusst, den Rücken freigehalten haben und genau wie meine Freund*innen immer da sind, wenn ich sie brauche.

Das Gleiche gilt auch für meine Mutter, die diese Worte leider nicht mehr lesen kann.